Estuarine, Coastal and Shelf Science 259 (2021) 107460

Contents lists available at ScienceDirect

Estuarine, Coastal and Shelf Science

journal homepage: www.elsevier.com/locate/ecss

Subtidal macrophyte diversity and potentials in Nha Trang Bay - baseline data for monitoring a rising natural resource

A. Fricke [a,b,*], X.V. Nguyen [c,d], M. Stuhr [a,e,f], T.D. Hoang [c], V.H. Dao [c,d], M.D. Tran [g], T.S. Pham [g], H.C. Le [h], M.H. Le [h], Q.L. Pham [h], M. Schmid [a], A. Kunzmann [a], A. Gärdes [a,i,j], J. von Hagen [k], M. Teichberg [a]

[a] Leibniz Centre for Tropical Marine Research (ZMT), Fahrenheitstrasse 6, 28359 Bremen, Germany
[b] Leibniz Institute of Vegetable and Ornamental Crops (IGZ), Theodor-Echtermeyer-Weg 1, 14979, Großbeeren, Germany
[c] Institute of Oceanography, Viet Nam Academy of Science and Technology, 01 Cau Da, Nha Trang City, Viet Nam
[d] Graduate University of Science and Technology, 18 Hoang Quoc Viet, Cau Giay, Ha Noi, Viet Nam
[e] Interuniversity Institute for Marine Sciences (IUI), P.O.B. 469, Eilat 88103, Israel
[f] Bar-Ilan University (BIU), Ramat Gan, Israel
[g] Nha Trang Institute of Technology Research and Application, Viet Nam Academy of Science and Technology, 02 Hung Vuong, Nha Trang City, Viet Nam
[h] Institute of Natural Products Chemistry, Viet Nam Academy of Science and Technology, 18 Hoang Quoc Viet, Cau Giay, Ha Noi, Viet Nam
[i] Alfred Wegener Institute for Polar and Marine Research, Department of Biosciences, Polar Biological Oceanography, Am Handelshafen 12, 27570, Bremerhaven, Germany
[j] University of Applied Sciences Bremerhaven, An der Karlstadt 8, 27570, Bremerhaven, Germany
[k] Merck KGaA, Darmstadt, Germany

ARTICLE INFO

Keywords:
Macroalgal diversity
Seagrass beds
Benthic harmful algal blooms (BHABs)
Light attenuation coefficient (Kd)
Sediment characteristics
Bioactive compounds
Viet Nam
Khánh Hòa
Nha Trang Bay

ABSTRACT

Tropical coastal ecosystems provide a unique complex marine habitat with a high diversity of algal species, Viet Nam being a particular hotspot. These algae may host a variety of potential unknown or underestimated bioactive algal compounds. In parallel the worldwide rising interest in macroalgae-based products leads to increasing activities in seaweed natural harvest and mariculture within coastal waters. With this growing interest, the present work provides baseline data for a systematic and science-based macroalgal monitoring program in Nha Trang Bay, Viet Nam, to keep track of potentially interesting taxa and to identify driving environmental factors which may also naturally influence biodiversity and species abundance. The present study investigated macrophyte diversity and abundance by combining a qualitative and quantitative macroalgal survey approach with environmental sampling (e.g. physicochemical properties of water column, underwater light regime, and sediment characteristics). Surveys were performed in the dry season (May/June) 2019 in different water depths (3, 6 and 10 m) at seven sites within Nha Trang Bay. The study revealed a coastal patchwork of diverse habitats inhabited by complex macrophyte communities, including estuarine dense *Sargassum* forests and *Turbinaria* meadows, sheltered sandy seagrass (*Halodule* spp.) beds with upcoming *Lyngbya* blooms, low diverse *Padina* deserts and highly turbid aquaculture (lobster and fish farms) impacted sites with surprisingly high macroalgal diversity. During our study a total of 86 macrophyte species were encountered in the subtidal (>1 m water depth), whereas only 6 species (*Padina australis*, *Sargassum mcclurei*, *Turbinaria ornata*, *Halimeda discoidea*, *Amphiroa fragilissima, Tricleocarpa cylindrical*) were frequently found at every survey site. The observed high patchiness and presence of economically important (e.g. *Sargassum* spp., *Gracilaria* spp., *Caulerpa* spp., *Gelidiella acerosa*, *Acanthophora spicifera*) and potentially economically interesting (e.g. *Padina australis*, *Turbinaria ornata*, *Stypopodium zonale*, *Chondria armata*) taxa during the survey underlines the high potential of the present macrophytic bio-resource, which apparently is strongly structured and will be altered by the changing heterogenic environment.

* Corresponding author. Leibniz Institute of Vegetable and Ornamental Crops (IGZ), Theodor-Echtermeyer-Weg 1, 14979, Großbeeren, Germany.
E-mail address: fricke@igzev.de (A. Fricke).

https://doi.org/10.1016/j.ecss.2021.107460
Received 2 October 2020; Received in revised form 5 May 2021; Accepted 31 May 2021
Available online 7 June 2021

1. Introduction

Over the past decade increasing interest in macroalgae-based products from different industries has led to high demands for the natural stock of commercialized taxa (FAO, 2018). Next to the application of rather unprocessed thalli for food and feed, there is a growing interest in algal-based bioactive extracts for the cosmetics, pharmaceutical and energy industry. Macroalgae provide a valuable source of protein and polysaccharides (e.g. carrageenan, agar, alginic acid, fucoidan), are rich in macro- and micronutrients (e.g. Vitamins, Omega-3) and provide different secondary metabolites reported to show a variety of bioactive effects (e.g. anti-oxidant, anti-inflammatory, anti-bacterial, anti-viral, anti-cancer) (Gnanavel et al., 2019; Ha et al., 2019; Tanna and Mishra, 2018).

Given their high diversity and morphological plasticity, macroalgae provide a high potential of so far undiscovered or underestimated novel compounds of which production can be triggered by different intrinsic and extrinsic factors. Characterized by complex life cycles with partly extreme heterogenic life stages and alterations in genetic ploidy levels, algal physiology can be strongly altered by complex abiotic and biotic parameters, including epi-or endophytic relations (Fricke et al., 2011), grazing pressures (Puk et al., 2020), nutrient limitations or enrichments (Teichberg et al., 2013) shifts in light regime (Fricke et al., 2014), substrate availability (Diaz-Pulido and McCook, 2004) and many more. Macroalgae provide a variety of physical (e.g. thallus sloughing; Littler and Littler, 1999) and chemical acclimation and defense mechanisms (Pereira and da Gama, 2008) in response to changing environmental conditions, which can alter their morphology and chemistry, including commercially interesting secondary compounds. In this respect there is an urgent need to better understand how the environment influences algae biodiversity, composition, and abundance, and how this may influence their potential use as a rising natural resource in a sustainable way.

The 3260 km long coast line of Viet Nam is characterized by a diverse climate ranging from tropical to temperate zones and provides a macroalgal hot-spot with over 700 macroalgal species listed (Nguyen et al., 2013). Within Viet Nam, the Nha Trang Bay (Fig. 1A) on the South-Central coast is known for its traditional algal harvest activities and biodiversity.

Approximately half of the number of known Vietnamese species are recorded for the Khánh Hòa province (Nguyen et al., 2013). The region forms a unique environment, given the observable high habitat heterogeneity, driven by e.g. the influx from the Cua Be and Cai rivers, island formations, water currents and seasonal monsoon and storm events, which may be a source for a variety of potentially unknown or underestimated algal compounds. In fact, about 481 macroalgal species have been recorded in the Bay, including 275 Rhodophyta, 121 Chlorophyta and 85 Ochrophyta over the past decades (Titlyanov et al., 2015). Favored for its mild climate, sandy beaches and a highly demanded local seafood kitchen, Nha Trang Bay faces increasing anthropogenically driven land-use changes including sedimentation by coastal constructions, eutrophication by human settlings, farming and aquaculture, and rising tourism activities.

Macroalgal harvesting and cultivation activities are expected to increase in the next years in the region due to rising interest in local derived algal products for the food industry. To date, main harvests in

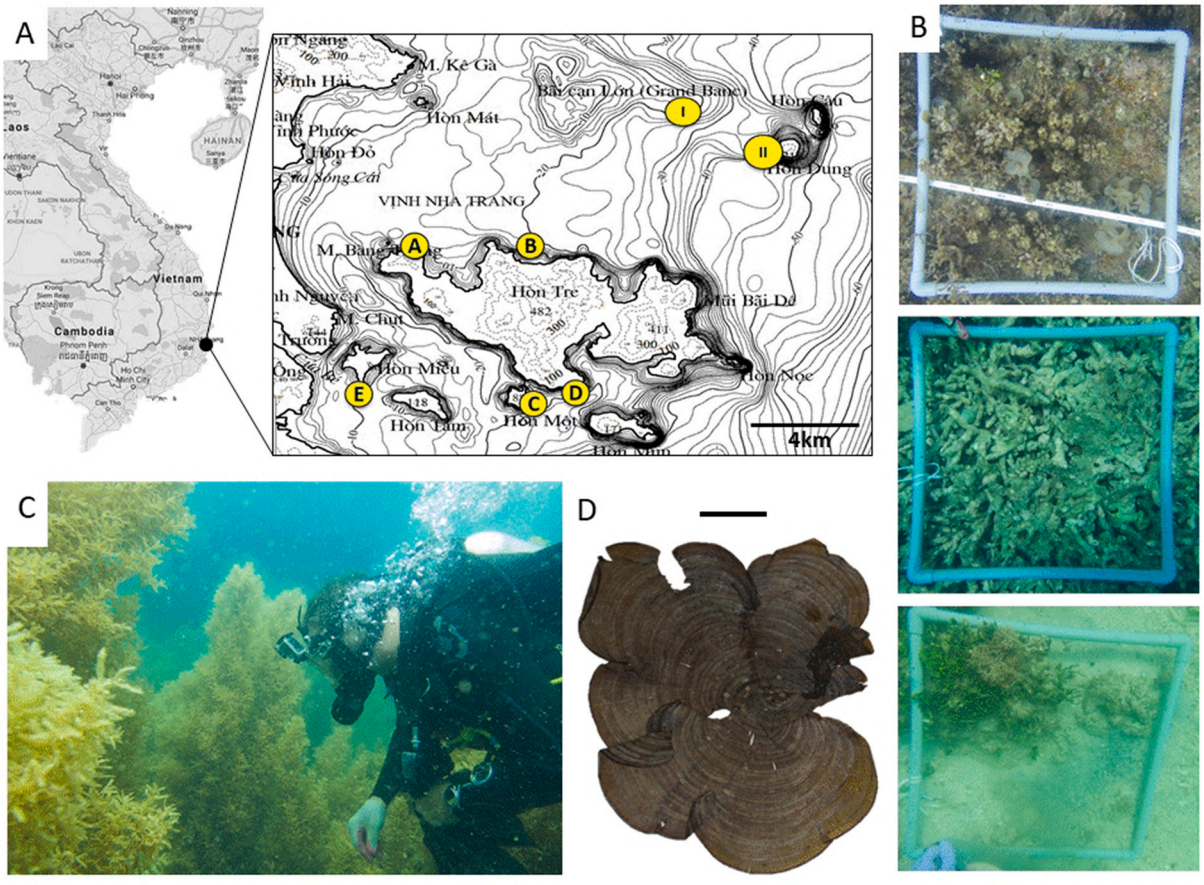

Fig. 1. A) Map showing position of survey sites (A–E) and additional collection sites (I, II) within the Nha Trang Bay, Viet Nam (details given in Appendix Table 1); B) Examples of 0.25 m^2 photo-quadrats taken at different sites (A, D and E) at 3 m water depths; C) *Sargassum* belt at Site B in 3–5 m water depth and D) Example of an herbarium sheet showing *Padina australis* prepared from collected algal material, incorporated in the herbarium of the institute of Oceanography Nha Trang. Scale bar corresponds to 2 cm.

the bay were primarily driven by cropping of the fleshy biomass of *Sargassum* spp. and numerous agarophytes, including *Hydropuntia, Gracilaria,* and *Gelidiella*, collected at low tide (Nguyen et al., 2013). In particular, growing demands for *Sargassum* biomass strongly increased harvest frequency and altered harvest mode (damaging removal instead of controlled cuttings) leading to a strong decline in the natural *Sargassum* beds over the past decade (Nguyen and Nguyen, 2011; Titlyanov et al., 2012).

Given the increasing pressure of human driven land-use changes and harvest activities, there is an urgent need to learn more about the present macroalgal community structure and biodiversity, its distribution and its ecological and potential economic value. It is also crucial to have baseline data of potentially commercially important species in order to sustainably manage resource use. The marine protected area (MPA) in Nha Trang Bay was founded in 2002 to maintain the inviting natural landscape with the assistance of the World Conservation Union and with funding of the GEF/World Bank and DANIDA (Doan Dung, 2007). The present work presents baseline data for future implementation of a macroalgal monitoring program for the Nha Trang Bay, allowing the surveillance of potentially interesting taxa and to identify driving environmental factors which may also naturally influence biodiversity and species abundance aside from harvesting. Five different sites characterized by heterogenic environmental conditions from pristine to impacted by human activities (e.g. construction activities, nutrient inputs nearshore, and recent implementation of lobster farms) were selected within the Nha Trang Bay and surveyed in a comparative manner via SCUBA diving. Qualitative and quantitative studies of macrophytic species biodiversity and abundance were investigated along with environmental parameters potentially affecting algal physiology and triggering the concentration of secondary metabolites. Thus, nutrients and underwater light regime were considered as key factors and approached in different ways – by setting three sampling depths (3, 6 and 10 m) and measuring the light profile, physicochemical properties of the water column (e.g. nutrient concentrations, turbidity, conductivity etc.) and surface bottom sediment characteristics (e.g. organic nutrient contents, stable isotope signatures) at each site. The present work provides, therefore, not only a quantitative snap shot of algal composition and diversity in the region, but also a valuable baseline for further macroalgal survey work imperative for future management of these valuable natural resources.

2. Material and methods

2.1. Collection sites

The Nha Trang Bay is characterized by rich and diverse underwater habitats, including coral reefs (Kunzmann et al., 2012; Tkachenko, 2015), seagrass beds (Nguyen et al., 2021) and *Sargassum* forests (Nguyen and Nguyen, 2011; Titlyanov et al., 2012), affected by the influx from the connected Cua Be and Cai rivers and different anthropogenic activities in the Bay (Du and Kunzmann, 2015). Macrophytes in the Bay profited from diverse, heterogenic hard substrates, including coral rubble, stones and artificial construction material (Titlyanov and Titlyanova 2013**).** To investigate the composition and distribution of macrophytes within Nha Trang Bay, a benthic biodiversity and abundance survey has been conducted during the dry season from May 3 to 5 and June 11 to 17 2019 (see Map, Fig. 1A). Five different sites were surveyed for the presence and distribution of their macroalgal community (Appendix Table 1).

The chosen sites were located around the main Hòn Tre Island in different distances to the Cua Be river estuary and characterized by different anthropogenic impacts. Site A (N 12°13.848′, E 109°14.505′) is the former place of lobster cages, left in 2018 due to converting and expanding the Vinpearl Land resorts, hotels and entertainment parks; site B (N 12°13.762′, E 109°16.894′) is situated close to a coastal construction site, connected to touristic leisure activities; site C (N 12°10.733‘, E 109°16.662‘) is a more remote open/unsheltered site with a steep rocky shore and a very sandy slowly dropping bottom close to the small island Hòn Môt, which has no major land-based activities; site D (N 12°10.947‘, E 109°17.585’), considered as a pristine site, is furthest away from the mainland located in a sheltered shallow sandy bay with short seagrass meadows, regularly visited by tourist boats; and site E (N 12°11.010‘, E 109°13.389‘) is situated close to an open-water lobster farming place, lying within a direct tourist boat traffic line and affected by smaller boats that short-cut their way over the shallow water. In addition to the survey two more sites were visited and sampled to study their macroalgal diversity: site I (N 12°17.007‘, E 109°18.936‘) is situated on an underwater plateau Bai Can Lon (“Great Bank”) which is known to support rich algal growth in spring season within close proximity; site II (N 12°16.425’, E 109°21.389′) is situated on the slope farther out Hon Dung Island. In relation to the MPA in the Nha Trang Bay, most sites (A-E) are situated in the MPA buffer zone shown by (Doan Dung, 2007, Fig.1.2), whereas site II comprises a sanctuary area and site I is completely outside the MPA. The field surveys from the above described sites were permitted by the People’s Nha Trang City in response to letters from the Institute of Oceanography, Viet Nam.

2.2. Sampling strategy

2.2.1. Environmental conditions

2.2.1.1. Weather data. Weather data (air temperature, relative humidity and rainfall) were gathered from the Department of Marine Physics, Institute of Oceanography and South-central regional hydrometeorological center at Nha Trang City for the month of June 2019, during the time of the quantitative survey (see below).

2.2.1.2. Water column parameters. Water column samples were taken in May and June 2019 at high tide (Appendix Table 1) parallel to macroalgal sample collections and survey activities at the different sites. Water samples were collected from the surface (n = 3) and bottom water layers (n = 3) using a 5L-Niskin sampling bottle (Ocean Test Equipment, INC, USA). Collected water was split to analyze i) total suspended solids (TSS), ii) chlorophyll *a* concentration (Chl *a*), in June sampling only and iii) nutrient concentrations in the water column. For analysis of TSS, 1 L of water was filtered through pre-combusted and weighed Whatman GF/F filters (pore size: 0.7 μm; diameter: 47 mm). Replicate filters were dried to weight constancy and its weight defined (lost and retained weights), weight was determined with high precision analytical scales (d = 0.0001 g, Sartorius, Germany). For Chl *a*, 1 L of seawater was filtered through a Whatman GF/F filter and kept frozen at −20 °C and dark until analyses. Chl *a* concentrations were analyzed by spectrophotometric methods after extraction in 90% acetone using a standard protocol (Parson et al., 1984). For nutrients, water samples were stored in 50-ml PE bottles and kept frozen until analyses. Dissolved inorganic nutrients were analyzed for dissolved inorganic nitrogen-DIN (NH_4–N, NO_2–N, NO_3–N) and phosphate (PO_4–P) by UV–visible spectrophotometer (Hitachi U-2900, Japan) (Parsons et al., 1984). Unfortunately, for site B only nutrient analyses for surface samples were realizable.

In addition, environmental measurements were taken with two different multi-parameter probes: a Multi 3630 (WTW by Xylem, Germany) for surface water and a Manta 2 (Eureka) to measure along a depth gradient (1–5 m) to determine temperature [°C], conductivity [mS cm^{-1}], salinity [PSS], pH, oxygen saturation and concentration [% Sat and mg L^{-1}], and turbidity [NTU] at each sampling site. Furthermore, to evaluate the underwater light regime, light measurements were taken along a depth gradient at each sampling site using a LICOR quantum sensor LI-190R (LICOR, USA) to measure Photosynthetically Active Radiation (~400–700 nm = PAR, in μmol of photons $m^{-2}s^{-1}$) and an integrated hyperspectral radiometer Ramses ACC UV/VIS (Trios, Germany) to measure light spectra between 280 and 720 nm with a

Table 1
Overview of macrophyte species encountered during summer (May/June) 2019 in the subtidal (>1 m) at different survey sites (A-E) and additional sites (I and II) in the Nha Trang Bay. Species are numbered according to their taxonomic grouping to Chloropyta (C1–C19), Ochrophyta (O1–O22), Rhodophyta (R1-R41), Trachaeophyta (T1-T2) and Cyanobacteria (Cy1-Cy2). Superimposed stars indicate presence of species in the quantitative abundance survey in June 2019. Species presence is presented for each site, for survey sites (A-E) sampling depths (3, 6, 10m) are provided, whereas crosses indicate verified sampling depth during survey and question marks indicate highly likely sampling depth during scouting activities. Frequency (F) indicates frequency of species sampled at surveyed sites (A-E). For the additional sites (I and II) water depths is provided in brackets.

	Sites	A				B				C				D				E					I	II
N°	Species/ Depths		3	6	10		3	6	10		3	6	10		3	6	10		3	6	10	F	10	10
Phyllum: Chlorophyta		7				5				5				6				13					2	1
Order: Bryopsidales																								
Family: Caulerpaceae																								
C1*	*Caulerpa chemnitzia* (Esper) J.V. Lamouroux																	1	?	X		1		
C2*	*Caulerpa racemosa* (Forsskål) J. Agardh									1	?							1	?		X	2		
C3	*Caulerpa racemosa* var. *macrophysa* (Sonder ex K ü tzing) W.R. Taylor	1	?															1	?			2		
C4*	*Caulerpa serrulata* (Forsskål) J. Agardh	1	?											1	?			1	?	X		3	1	
C5	*Caulerpa verticillata* J.Agardh 1847													1	?							1		
Family: Codiaceae																								
C6	*Codium geppiorum* O.C.Schmidt																	1	X			1		
Family: Dichotomsiphonaceae																								
C7	*Avrainvillea erecta* (Berkeley) A. Gepp & E.S.Gepp													1	?							1		
Family: Halimedaceae																								
C8*	*Halimeda discoidea* Decaisne	1	X			1	X			1	?			1	X			1	X	X	X	5		
C9	*Halimeda macroloba* Decaisne																						1	
C10*	*Halimeda opuntia* (Linnaeus) J.V. Lamouroux	1	X	X										1	X			1	X	X	X	3		
C11*	*Halimeda velasquezii* W.R.Taylor	1	X			1	X	X										1	X			3		
C12	*Halimeda cuneata* Hering	1	?			1	?			1	?							1	?	?		4		
Family: Udoteaceae																								
C13	*Rhipidosiphon javanensis* Montagne																							*1*
Order: Cladophorales																								
Family: Boodleaceae																								
C14	*Avrainvillea erecta* (Berkeley) A. Gepp & E.S.Gepp													1	?							1		
C15	*Boodlea composita*(Harvey) F. Brand	1	?			1	?			1	?							1	?			4		
Family: Siphonocladaceae																								
C16*	*Dictyosphaeria versluysii* Weber Bosse					1	?			1	X											2		
Family: Valoniaceae																								
C17	*Valonia ventricosa* J.Agardh																	1	?			1		
Family: Dasycladaceae																								
C18*	*Bornetella nitida* Munier-Chalmas ex Sonder																	1	X			1		
C19	*Bornetella oligospora* Solms-Laubach																	1	?			1		
Phyllum: Ochrophyta		14				13				8				10				14					5	2
Order: Dictyotales																								
Family: Dictyotaceae																								
O1	*Canistrocarpus cervicornis* (Kützing) De Paula & De Clerck in De Clerck et al.					1	?															1		
O2	*Canistrocarpus crispatus* (J.V. Lamouroux) De Paula & De Clerck					1	?															1		
O3*	*Dictyota dichotoma* (Hudson) J. V.Lamouroux	1	?			1	X							1		X		1		?	X	4		
O4*	*Dictyota friabilis* Setchell													1	X			1	X			2		
O5*	*Dictyota* spp.	1	X			1	?			1	X	X						1	?					
O6*	*Lobophora variegata* (J.V. Lamouroux) Womersley ex E.C. Oliveira	1	X			1	X	X	X	1	X		?					1	X			4		*1*
O7*	*Padina australis* Hauck	1	X	X	X	1	X			1	X	X	X	1	X	X	X	1	X	X	X	5	1	*1*
O8*	*Padina minor* Yamada													1	X			1	X	X		2		
O9	*Spatoglossum vietnamense* Pham-Hoàng Hô					1	X															1		
O10*		1	?	X	X																	1	1	

(*continued on next page*)

Table 1 (*continued*)

	Sites	A			B			C			D				E					I	II
	Stypopodium zonale (J.V. Lamouroux) Papenfuss																				
Order: Ectocarpales																					
Family: Scytosiphonaceae																					
O11*	*Colpomenia sinuosa* (Mertens ex Roth) Derbès & Solier	1	X		1	?													2	1	
O12*	*Hydroclathrus clathratus* (C. Agardh) M.Howe	1	?		1	?					1	?			1	X			4		
O13*	*Pseudochnoospora implexa* (J. Agardh) Santiañez, G.Y.Cho & Kogame	1	?					1	X		1	X	X		1	X	?	X	4	1	
Order: Fucales																					
Family: Sargassaceae																					
O14	*Hormophysa cuneiformis* (J.F. Gmelin) P.C.Silva	1	?					1	?										2		
O15	*Sargassum aquifolium* (Turner) C. Agardh	1	?		1	?													2		
O16	*Sargassum denticarpum* Ajisaka														1	?			1		
O17	*Sargassum herklotsii* Setchell														1	?			1		
O18*	*Sargassum ilicifolium* (Turner) C. Agardh	1	X																1		
O19*	*Sargassum mcclurei* Setchell	1	?		1	?		1	?		1	?	X		1	?			5	1	
O20*	*Sargassum polycystum* C.Agardh										1	X			1	?			2		
O21*	*Sargassum* spp.	1	X	X	1	X	X	1	X	X	1	X		X	1	X					
O22*	*Turbinaria ornata* (Turner) J. Agardh	1	X		1	X	X	1	?		1	X		X	1	?			5		
Rhodophyta		19			16			16			13				26					5	1
Order: Bonnemaisoniales																					
Family: Bonnemaisoniaceae																					
R1*	*Asparagopsis taxiformis* (Delile) Trevisan				1	X													1	1	
Order: Ceramiales																					
Family: Delessariaceae																					
R2	*Claudea batanensis*Tanaka																			1	
Family: Laurencieae																					
R3*	*Laurencia obtusa* (Hudson) J.V. Lamouroux										1	X							1		
R4 *	*Laurencia* sp.	1	X		1	?		1	X	X	1	X							4		
R5	*Palisada concreta* (A.B.Cribb) K. W.Nam							1	?						1	?			2		
R6*	*Palisada parvipapillata* (C.K. Tseng) K.W.Nam	1	X								1	X			1	X			3		
Family: Rhodomelaceae																					
R7*	*Acanthophora spicifera*(M.Vahl) Børgesen	1	?		1	?									1	X			3		
R8	*Chondria armata (Kützing)* Okamura																				*1*
R9*	*Leveillea jungermannioides* (Hering & G.Martens) Harvey				1	?									1	X			2		
R10*	*Polysiphonia* sp.							1	X										1		
Order: Corallinales																					
Family: Corallinaceae																					
R11*	*Cheilosporum* sp.				1	x									1	x			2		
R12	*Jania adhaerens* J.V.Lamouroux	1	?		1	?									1	?			3		
R13*	*Jania* sp.	1	X								1	?							2		
Family: Lithophyllaceae																					
R14*	*Amphiroa foliacea* J.V. Lamouroux	1	X		1	?		1	X						1	X			4		
R15*	*Amphiroa fragilissima* (Linnaeus) J.V.Lamouroux	1	X		1	X		1	X	X	1	?			1	X			5		
R16	*Amphiroa* sp.	1	?																1		
Order: Gelidiales																					
Family: Gelidiellaceae																					
R17*	*Gelidiella* sp.	1	X	X															1		
R18*	*Gelidiella acerosa* (Forsskål) Feldmann & Hamel														1	X			1		
R19*	*Gelidium* sp.				1	X					1	?			1	?	?	?	3		
Order: Gigartinales																					
Family: Cystocloniaceae																					
R20*	*Hypnea anastomosans* Papenfuss, Lipkin & P.C.Silva	1		X							1	X			1	X	X		3		
R21*	*Hypnea pannosa* J.Agardh	1	X					1	?		1	?			1	?	X		4		
R22	*Hypnea valentiae* (Turner) Montagne														1		X		1		
R23*	*Hypnea* sp.	1	?		1	x		1	?						1	?	X		4		

(*continued on next page*)

Table 1 (*continued*)

	Sites	A		B		C		D			E					I	II
Order: Gracilariales																	
Family: Gracilariaceae																	
R24*	*Gracilaria arcuata* Zanardini										1	X			1		
F25	*Gracilaria salicornia* (C.Agardh) E.Y.Dawson																
R26*	*Hydropuntia edulis* (S.G.Gmelin) Gurgel & Fredericq					1	?	1	X		1	X			3		
R27	*Hydropuntia eucheumatoides* (Harvey) Gurgel & Fredericq	1	?	1	?	1	?				1	?			4		
Order: Halymeniales																	
Family: Halymeniaceae																	
R28	*Halymenia dilatata* Zanardini			1	?	1	?				1	?			3		
R29*	*Prionitis formosana* (Okamura) Kawaguchi & Nguyen	1	X	1	?	1	?								3		
Order: Nemaliales																	
Family: Galaxauraceae																	
R30*	*Actinotrichia fragilis* (Forsskål) Børgesen	1	?	1	?	1	?	1	X						4		
R31*	*Dichotomaria marginata* (J.Ellis & Solander) Lamarck															1	
R32*	*Galaxaura filamentosa* R.C.Y. Chou					1	X				1	?			2		
R33*	*Galaxaura* sp.					1	?	1	X		1	X			3		
R34*	*Tricleocarpa cylindrica* (J.Ellis & Solander) Huisman & Borowitzka	1	?	1	?	1	X	1	X		1	X			5	1	
Family: Liagoraceae																	
R35	*Dernonema* sp.	1	?												1		
R36	*Liagora* sp.										1	?			1		
Order: Nemastomatales																	
Family: Schizymeniaceae																	
R37	*Titanophora weberae* Børgesen	1	?	1	?	1	?				1	?			4	1	
Order: Peyssonneliales																	
Family: Peyssonneliaceae																	
R38*	*Peyssoniella* sp.	1	X				?				1	?	?	?	2		
Order: Rhodymeniales																	
Family: Champiaceae																	
R39	*Champia parvula* (C.Agardh) Harvey							1	?						1		
Family: Hymenocladiaceae																	
R40*	*Asteromenia anastomosans* (Weber Bosse) G.W.Saunders, C. E.Lane, C.W.Schneider & Kraft										1	X			1		
R41	*Ceratodictyon intricatum* (C. Agardh) R.E.Norris										1	X			1		
Phyllum: Tracheophyta								2									
Order: Alismatales																	
Family: Cymodoceaceae																	
T1	*Halodule pinifolia* (Miki) Hartog							1		X X					1		
Family: Hydrocharitaceae																	
T2	*Halophila major* (Zollinger) Miquel							1		X X					1		
Phyllum: Cyanobacteria								1			1						
Order: Oscillatoriales																	
Family: Oscillatoriaceae																	
Cy1	*Lyngbya* cf. *majuscula*							1	X	X X					1		
Cy2	*Oscillatoriaceae*										1	X			1		
TOTAL		40		34		29		32			54					12	4

wavelength accuracy of 0.2 nm. Light measurements were taken directly above the water (0 m), at the surface (0.1 m) and down the water column in 0.5 m intervals. Maximum depths were restricted by anchoring depths during sampling events. A minimum of two replicates were taken for each light transect measurement. Transparency for UVB (280–320 nm), UVA (320–400 nm) and PAR (400–700 nm) was calculated as % of the average of the correspondent surface radiation (0 m), considered as 100%, for all measured depths. In addition, the diffuse attenuation coefficients Kd (m^{-1}) were calculated for the (LICOR) PAR values following (Hanelt et al., 2001; Kirk, 1994) using the formula:

$$Iz = I0e^{-Kd(PAR)*z}$$

where Iz = irradiance at the depth z, $I0$ = irradiance just below the surface and the euphotic depth = depth in the water column. Kd was calculated in 1 m steps for the upper 3 m water column at each site. As Kd is a logarithmic derivative, low Kd of about 0.1 m^{-1} indicate about 10% light attenuation per meter, whereas Kd values of about 1 m^{-1} indicate very turbid waters. The corresponding euphotic depth was also calculated where 1% of the 100% PAR surface irradiance occur and theoretically the limit of photosynthetic life is expected.

2.2.1.3. Sediment samples (chemistry, grain size and composition). A bulk sediment sample was collected parallel to the survey at each sampling depth (3, 6 and 10 m) at sites A-E and at the bottom depths at site I (8 m) and II (10 m). The uppermost ~1 cm of sediment was carefully collected by scientific divers into pre-labelled zip-lock bags, brought to the surface and stored in cold and dark conditions. At the Institute of Oceanography, the sediments were air-dried until transportation to the ZMT in Bremen where they were dried again for 72 h at 40 °C. The sediment samples were split (Fema-Salzgitter, Münster) and one half of each sample was ground to powder (FRITSCH premium line pulverisette 7) for bulk sample analysis of the organic carbon (C_{org}) and nitrogen (N) contents and for determination of stable carbon and nitrogen isotope ratios. The other half was investigated for sediment composition using a digital microscope (Premier AM4113ZT, Dino-Lite) to photograph, visually inspect and describe the dried bulk sediment samples on a dark sample tray.

C and N was analyzed via a CHN elemental analyzer (Eurovector Euro EA 3000, precision calculated from analysis of standards: 1.61% ± 0.09 for C and 0.133% ± 0.023 for N) from 20 ± 1 mg of ground dried samples filled into tin cups. POC measurements were determined from 30 ± 1 mg sediment powder filled into silver cups, pre-treated with 350 µl 1 N HCL and re-dried at 40 °C for 72 h prior to analysis. Carbon and nitrogen isotope ratios of the bulk sediment powder were determined using an elemental analyzer coupled with an isotope ratio mass-spectrometer (Delta Plus flash EA 1112, Thermo Finnigan). The derived results of isotope ratios are expressed in standard δ-unit notation, which is defined as: $\delta^{13}C$ or $\delta^{15}N = [(R_{sample}/R_{standard}) - 1] \times 1000‰$, where R is the $^{13}C/^{12}C$ or the $^{15}N/^{14}N$ ratio. The values were reported relative to the Vienna Pee Dee Belemnite (PDB) standard. A laboratory working standard (peptone) was run for every 7 samples. Analytical precision was ±0.1‰. All C_{org}/N and stable isotope measurements were performed in triplicates and averaged for further analyses.

2.2.2. Qualitative macroalgal diversity survey

To study the macroalgal diversity based on presence and absence at the survey sites (A-E) and the additional visited sites (I and II), macroalgae were collected in the shallow subtidal between 1 and 5 m water depths via snorkeling and SCUBA diving in May 2019 and in June 2019 in parallel with the abundance survey activities in the shallow subtidal (1–5 m) at the sites A-E.

2.2.3. Quantitative macroalgal diversity and abundance survey

To quantify the macrophytic community in terms of species diversity and abundance within the surveyed areas (A-E), survey transects were conducted via SCUBA diving at the three reference depths 3, 6 and 10 m at each site in June 2019. Depths were adjusted according to prior field observations and experience, whereas the maximum water depth of 10 m was oriented to the water depth of site I, known to support seasonal macroalgal stocks, and the shallowest depth (3 m) provided intended subtidal conditions, where SCUBA diving was needed for an accurate investigation and the 6 m water depth was set in between.

For orientation a 10-m transect tape was deployed along the bathymetric contour of each reference depth following standard procedures. A sampling-quadrat (0.25 m^2) was positioned along this marker and randomly replicated 4 times. This procedure resulted in a total of 5 sites × 3 water depths x 4 replicates = 60 sampling quadrats. At each sampling event, photos of the quadrats were taken (Fig. 1C; DSC-RX100M3, Sony, equipped with an underwater case) and all macroalgae above > 1 cm height were removed by hand, transferred into mesh bags (mesh size < 1 cm) and brought to the surface. For a more detailed investigation of the macroalgal biodiversity, hard substrates (e.g. stones, rubble, nets etc.) encountered in the different photo-quadrats were additionally collected and analyzed for turf algal species (<1 cm) present. Materials were pre-sorted according to macroscopically distinguishable taxa and stored in moistened conditions until transfer to the facilities of the Institute of Oceanography.

2.3. Sample processing

2.3.1. Identification of species for species richness and biomass quantification

Microscopy-based morphological species analyses started within the same day of collection. Sections were made by hand and material was mounted in 50% corn syrup solution when necessary to aid in identification (Fricke et al., 2017). Photomicrographs were taken on an Olympus CH30 microscope (Tokyo, Japan) with a Q-imaging digital camera (Burnaby, BC, Canada), and habit views were reproduced with an Epson scanner (Tokyo, Japan). We used different literature for the morphological identification (e.g. Abbott et al., 2002; Pham-Hoang, 1969; Le and Nguyen, 2010; Nguyen, 2007). After identification, fresh weight was taken from each taxon and material was dried for a minimum of 3 days at 60 °C to weight constancy. Wet and dry biomass were calculated for each individual taxon. Total macrophytic biomass (g m^{-2}) was calculated from individual taxa dry weights. Additional sampling activities specimen sheets were prepared from each species encountered during the survey and incorporated into the collection of the Nha Trang Institute of Oceanography (herbarium of the Institute of Oceanography Nha Trang; Project TroMaCos – Marine Algae of Viet Nam 001 to 131). Sub-samples were taken from fresh material and preserved for further molecular investigations for cases where species identification strictly based on the morphological investigation was doubtful. The DNA extraction was carried out using the Quick-DNA™ Miniprep Plus Kit (Zymo Research, CA, USA) following the manufacturer's instructions.

2.3.2. Visual macrobenthic survey

Underwater photographs taken at the biomass-rich and diverse 3 m water depth were analyzed and compared to biomass data to evaluate the use of underwater photography as a non-destructive alternative for carrying out macroalgal surveys at the research sites. We used the 99 point count method with the software Coral Point Count with Excel extensions (CPCe) (Kohler and Gill, 2006) to determine relative abundance of taxa. Due to high dispersion from the sandy ground (site C and D) and high turbidity of the water column (site E), 6 of the 20 pictures were excluded for the evaluation. Photos were compared with biomass data to identify taxa and substrates of interest prior to analysis. For comparison, relative abundance was calculated for the macroalgal taxa from biomass and photo analyses by calculating percentage contribution of individual taxa to each analyzed community, and relative total abundances were calculated by adding up the corresponding values for each taxa.

2.4. Statistics

Nonparametric permutation analyses of variances (PERMANOVA) were applied using the software Primer v6 (+PERMANOVA package) to investigate differences in environmental data, taxa composition, species richness and total macrophyte biomass between sites (factor: site – A, B, C, D, E, I and II), sampling depths (factor: depth of 3, 6 and 10 m or surface vs. bottom samples) and sampling times (May vs. June). Euclidean distances were calculated for species richness, environmental, sediment data and total biomass, whereas later was log-transformed prior to analyses. Bray–Curtis similarity indices were calculated for biomass-based species abundance data and calculated relative abundance data. Data were square root- and log-transformed prior to analysis in order to scale-down the importance of the highly abundant taxa. To overcome the issue of a high number of missing taxa in the data set, dummy correction was applied with value = 0.001. Monte Carlo corrections were applied in pairwise PERMANOVA comparisons to improve the accuracy of the p-value given by a low number of sample replicates and limited number of possible permutations. Pairwise comparisons were combined with SIMPER analyses to identify the taxa responsible

for ≥60% of identified dissimilarity between significantly differing assemblages. To compare and visualize the differences in the multidimensional data sets, Non-metric Multi-dimensional Scaling plots (NMDS) were created. To investigate potential abiotic drivers for biomass growth and diversity, 3 m water depth was chosen as a marker depth for comparisons between sites due to the generally high macroalgal abundances found at this depth. Differences in species composition were visualized using principal coordinates (PCO) analyses based on Bray Curtis similarity matrices, calculated from log-transformed abundance biomass data. Pearson correlations of the environmental variables were identified to help to determine the main abiotic factors driving differences in algal composition. The considered environmental data included: water temperature, pH, salinity, HDO (mg/L), %UVB, %UVA and %PAR measured or calculated at 3 m water depth, nutrient concentrations for PO_4–P, NO_3–N and NO_2–N, TSS and Chl *a* measured in bottom waters in May and June, and sediment data compiled for all three depths. Correlations calculated with r > 0.75 were considered as vectors and displayed on the PCO.

3. Results

3.1. Environmental conditions

3.1.1. Temperature, rainfall, salinity, pH and light

In the present study air temperatures reached a monthly peak of 39.3 °C in June 11 (Fig. 2A) leading to a maximum water temperature of 32.4 °C (Fig. 2B) at site D and 30.9°C–31.6 °C across the other sites. Summerly monsoon activities were recorded during June 2019 (Fig. 2A), with maximum rainfalls of 3.8 mm, but were hardly observed during the survey (one event with 0.4 mm at June 13). The nearshore site A showed the lowest surface salinities of about 32.7 PSS, whereas highest values of 33.9 and 34 were measured further out at sites II and D, respectively (Fig. 2C, Appendix Table 2). Strong salinity depth gradients were measured at sites A, B and E, reaching highest salinity levels below 5 m water depths A (Fig. 2C, Appendix Table 2). For pH, highest values were measured in surface waters of site A (pH = 8.31), whereas lowest pH values were found in the neighbored site B (pH = 8.18). At the other sites, pH of surface waters ranged between 8.21 and 8.24 (Fig. 2D, Appendix Table 2).

Monsoon activities led to high variations in cloud cover marked by a decrease in 32% UVB, 35% UVA and 37% PAR between clear sky and >95% cloud cover (Fig. 3A). During the time of the study the average maximum values for PAR (400–700 nm) were 1927 ± 40 µmol, while those of UVB (280–320 nm) were 1.66 ± 0.02 mW m^{-2} and that of UVA (320–400 nm) were 37.86 ± 0.22 mW m^{-2}, recorded on June 12th, 2019. Light transparency strongly differed between the sites with significantly lowest overall light transparency measured at the nearshore site E, showing a reduction of 93% UVB, 78% UVA and 72% PAR at 3 m water depth (Fig. 3B–D), maximum Kd (PAR) values of 0.5 m^{-1} and calculated euphotic depths of p_E = 9–11 m (Fig. 3E). In comparison, about 8% surface PAR (62 µmol $m^{-1}s^{-1}$) were measured at 9 m water depths. In contrast, the outer sites Site II and D showed high light transparencies (Appendix Table 3) with reductions of 64% UVB, 24% UVA, 48% PAR and 75% UVB, 46% UVA, 55% PAR at 3 m water depth, maximum Kd values of 0.25 m^{-1} and 0.27 m^{-1} and calculated euphotic depths of p_{II} = 18–22 m and p_D = 17–30 m (Fig. 3E), respectively.

3.1.2. Water column nutrients and water quality

Nutrient concentrations in the water column significantly differed over time (PERMANOVA Pseudo-F = 7613, p > 0.001; Fig. 4, Appendix Table 4). PO_4–P peaked in May compared to June at 18 ± 8 µg L^{-1} and 7 ± 2 µg L^{-1}, respectively. NO_3–N also showed approximately 11 times higher concentrations in the preceding month (150 ± 4 µg L^{-1} in May compared to 14 ± 2 µg L^{-1} in June). In contrast, NO_2–N increased in June from May values (May: 0.9 ± 0.1 µg L^{-1}, June: 2.3 ± 0.3 µg L^{-1}). In general, nutrients measured in the surface water column did not differ substantially to the bottom water column samples. The only differences observed were in PO_4–P in May at the nearshore site A

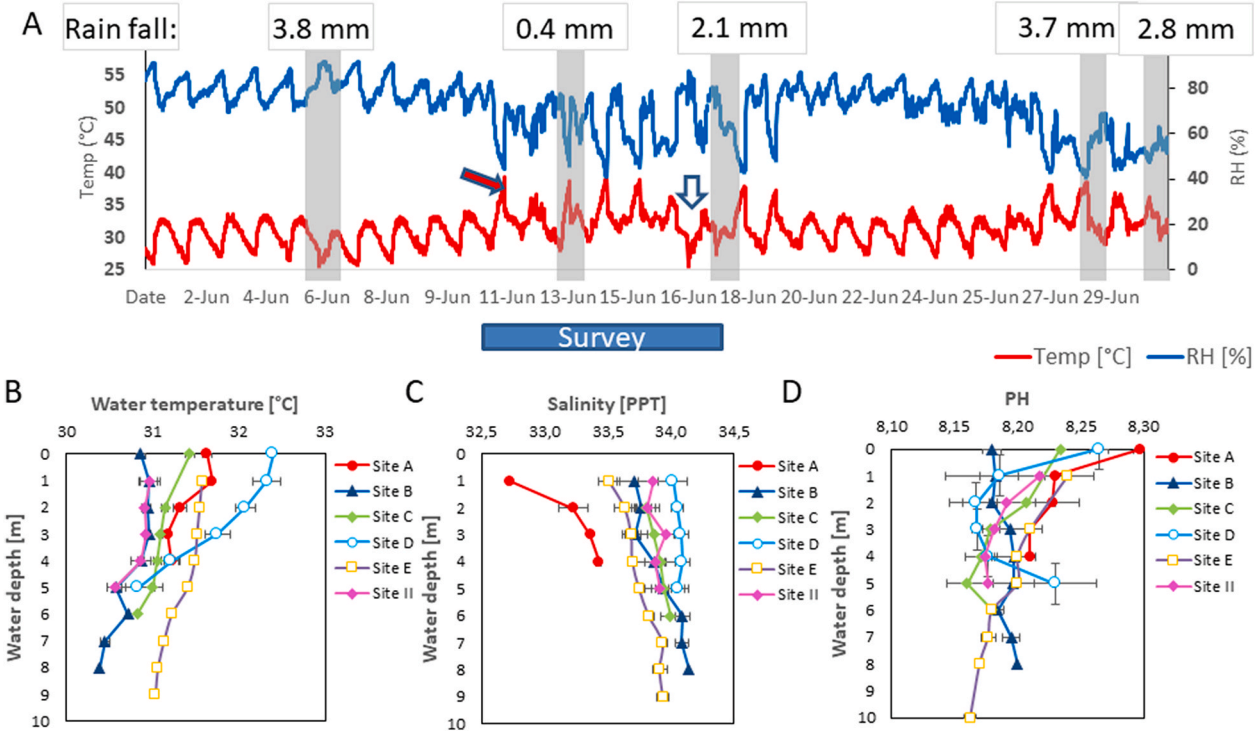

Fig. 2. A) Weather data of Nha Trang (rain fall, marked as grey bars) and neighboring Van Phong Bay (air temperature, marked as lower red line; relative humidity (RH), marked as upper blue line) in June 2019. Time of survey is indicated. Small arrows mark maximum air (red) and water (blue, at site C) temperature. Depth related differences in B) water, C) salinity and D) pH measured along depth gradients at different sites. Data showing mean ± S.D. Dates indicated in Appendix Table 1. (For interpretation of the references to colour in this figure legend, the reader is referred to the Web version of this article.)

Table 2
Differences in macroalgal composition of encountered taxa during the quantification abundance surveys at order and species level and of the six frequent taxa present at sites A-E (*Amphiroa fragilissima, Halimeda discoidea, Padina australis, Sargassum mcclurei, Tricleocarpa cylindrical, Turbinaria ornata)*. A) Results of 2-way PERMANOVAs and B) subsequent pairwise comparisons (Pairwise), showing differences in macroalgal composition between sites (factor: Site – A, B, C, D and E) and sampling depths (factor: Depth - 3, 6 and 10 m). Analyses based on dried biomass data of individual species/taxa, log-transformed prior to analyses, using Bray-Curtis distances. Results of SIMPER are given to each significant difference, showing percentage dissimilarity (% diss.) and listing algal taxa contributing to up to 60% cumulative differences; location of higher biomass or presence (only at) of listed taxa are provided, superimposed letters in species level indicate corresponding order (Ali = Alismatales, Bry = Bryopsidales, Cla = Cladophorales, Cor = Corallinales, Dic = Dictyotales, Ect = Ectocapales, Fuc = Fucales, Gra = Gracilariales, Osc = Oscillatoriales).

A) PERMANOVA

	Order level			Species level		Six frequent taxa	
	dF	Pseudo-F	P	Pseudo-F	p	Pseudo-F	p
Site	4	3.72	**0.001**	3.39	**0.001**	3.37	**0.001**
Depth	2	7.92	**0.001**	5.48	**0.001**	5.90	**0.001**
Site x Depth	8	1.85	**0.002**	1.94	**0.001**	1.68	**0.02**
Res	45						

B) PAIRWISE and SIMPER			
Depth differences at each site			
Site A:	3m≠6 (**p=0.02**; 81% diss.), 3m≠10m (**p=0.03**; 94% diss.)	3m≠6m (**p=0.03**; 90% diss.), 3m≠10m (**p=0.03**; 97% diss.)	3m≠6m (**p=0.03**; 88% diss.), 3m≠10m (**p=0.03**; 94% diss.)
	only at 3m: Corallinales	only at 3m: *Amphiroa fragilissima*^{Cor}, *A. foliaceae*^{Cor}, *Halimeda discoidea*^{Bry}, *Sargassum duplicatum*^{Fuc}, *Turbinaria ornata*^{Fuc}	only at 3m: *Amphiroa fragilissima*^{Cor}, *Turbinaria ornata*^{Fuc}
	3m > 6m: Fucales, Bryopsidales	6m > 3m > 10m: *Padina australis*^{Dic}	
	6m > 3m > 10m: Dictyotales		6m > 3m > 10m: *Padina australis*^{Dic}
Site B:	3m≠6 (**p=0.03**; 89% diss.), 3m≠10m (**p=0.02**; 93% diss.)	3m≠6m (**p=0.03**; 92% diss.), 3m≠10m (**p=0.04;**; 99% diss.)	3m≠6m (**p=0.02**; 96% diss.), 3m≠10m (**p=0.02;** 100% diss.)
	3m > 6m: Bryopsidales, Fucales	only at 3m: *Halimeda discoidea*^{Bry,} *Padina australis* ^{Dic}	only at 3m: *Halimeda discoidea*^{Bry}
		3m > 6m: *Sargassum* sp. ^{Fuc}, *Turbinaria ornata*^{Fuc}, *Halimeda velasquezii*^{Bry}	
Site C:	No difference	No difference	No difference
Site D:	3m≠10m (**p=0.03**; 93% diss.)	3m≠10m (**p=0.04**; 98% diss.)	No difference
	Only at 3m: Bryopsidales, Nemaliales	Only at 3m: *Halimeda opuntia*^{Bry}, *H. discoidea*^{Bry}, *Sargassum polycystum* ^{Fuc}	
	3m > 10m: Fucales	Only at 10 m: *Halophila major*^{Ali}	
	10m > 3m: Alismatales	10m > 3m: *Lyngbya* sp.^{Osc}	
Site E:	3m≠6m (**p=0.04**; 59% diss.)	3m≠6m (**p=0.04**; 80% diss.)	No difference
	only at 3m: Nemaliales, Ceramiales, Graciales	only at 3m: *Halimeda velasquezii*^{Bry}, *Oscillatoriaceae, Chondrophycus parvipallitus*^{CER}, *Hydropuntia edulis*^{Gra}, *Galaxaura* sp.^{Cor}, *Lobophora variegata*^{Dic}	
	3m > 6m: Bryopsidales	3m > 6m: *Halimeda discoidea*^{Bry}	
		6m > 3m: *Padina australis* ^{Dic}, *H. opuntia*^{Bry}	
Site differences at each depth			
In 3m			
A vs B	A≠B (**p=0.02**; 49% diss.)	A≠B (**p=0.02**; 64% diss.)	A≠B (**p=0.03**; 51% diss.)
	A > B: Fucales, Corallinales	Only in A: *Sargassum duplicatum*^{Fuc}, *Amphiroa foliaceae*^{Cor},	A > B: *Turbinaria ornata*^{Fuc}
	B > A: Bryopsidales	A > B: *Turbinaria ornata*^{Fuc}, *Amphiroa fragilissima*^{Cor,} *Padina australis*^{Dic}	B > A: *Halimeda discoidea*^{Bry}
		B > A: *Sargassum* sp.^{Fuc}, *Halimeda discoidea*^{Bry}	
A vs C	A≠C (**p=0.02**; 84% diss.)	A≠C (**p=0.03**; 90% diss.)	A≠C (**p=0.02**; 89% diss.)
	Only in A: Bryopsidales	Only in A: *Halimeda discoidea*^{Bry}, *Turbinaria ornata* ^{Fuc}, *Sargassum duplicatum*^{Fuc}	Only in A: *Turbinaria ornata* ^{Fuc}
	A > C: Corallinales, Fucales	A > C: *Amphiroa fragilissima*^{Cor}, *A. foliaceae*^{Cor}	A > C: *Amphiroa fragilissima*^{Cor}
		C > A: *Padina australis*^{Dic}	C > A: *Padina australis*^{Dic}
A vs D	A≠D (**p=0.04**; 73% diss.)	A≠D (**p=0.03**; 90% diss.)	No difference
	Only in A: Corallinales	Only in A: *Amphiroa foliaceae*^{Cor}, *A. fragilissima*^{Cor}, *Sargassum* sp.^{Fuc}, *S. duplicatum*^{Fuc}	
	A > D: Fucales, Bryopsidales	A > D: *Turbinaria ornata*^{Fuc}, *Halimeda discoidea*^{Bry}	
		Only in D: *Sargassum polycystum*^{Fuc}	
A vs E	A≠E (**p=0.02**; 71% diss)	A≠E (**p=0.03**; 81% diss.)	A≠E (**p=0.02**; 84% diss.)
	A > E: Fucales, Corallinales	Only in A: *Turbinaria ornata*^{Fuc}, *Sargassum duplicatum*^{Fuc}	Only in A*: Turbinaria ornata*^{Fuc}
	E > A: Bryopsidales	A > E: *Amphiroa fragilissima*^{Cor}, A. *foliaceae*^{Cor}, *Halimeda discoidea*^{Bry}, *H. velasquezii*^{Bry}, *Sargassum sp*^{Fuc}	A > E: *Amphiroa fragilissima*^{Cor}
		E > A: *Halimeda opuntia*^{Bry}	
B vs C	B≠C (**p=0.02**; 82% diss.)	B≠C (**p=0.03**; 89% diss.)	B≠C (**p=0.01**; 89% diss.)
	Only in B: Bryopsidales	Only in B: *Halimeda discoidea*^{Bry}, *H. velasquezii*^{Bry}	Only in B: *Halimeda discoidea*^{Bry},
	B > C: Fucales	B > C: *Sargassum* sp ^{Fuc}	C > B: *Padina australis* ^{Dic}
		C > B: *Padina australis* ^{Dic}	
B vs D	B≠D (**p=0.02**; 60% diss.)	B≠D (**p=0.03**; 85% diss.)	No difference
	B > D: Bryopsidales, Fucales	Only B: *Halimeda velasquezii*^{Bry}, *Sargassum* sp. ^{Fuc}	
		B > D: *Halimeda discoidea*^{Bry}	
		Only in D: *Sargassum polycystum*^{Fuc}, *Halimeda opuntia*^{Bry}	
B vs E	B≠E (**p=0.02**; 53% diss.)	B≠E (**p=0.02**; 76% diss.)	B≠E (**p=0.03**; 79% diss.)
	Only at E: Nemaliales	only B: *Turbinaria ornata*^{Fuc}	only B: *Turbinaria ornata*^{Fuc}
	B > E: Fucales, Bryopsidales	B > E: *Sargassum sp*^{Fuc}, *Halimeda discoidea*^{Bry}, *H. velasquezii*^{Bry}	B > E: *Halimeda discoidea*^{Bry}
		only E: *Halimeda opuntia*^{Bry}, *Chondrophycus parvipapillatus*^{Cer}	
C vs D	No difference	No difference	No difference
C vs E	No difference	C≠E (**p=0.03**; 90% diss.)	No difference

(*continued on next page*)

Table 2 (*continued*)

		only in E: *Halimeda opuntia*[Bry], *H. discoidea*[Bry], *H. velasquezii*[Bry], *Chondrophycus parvipapillatus*[Cer], *Hydropuntia edulis*[Gra], *Galaxaura* sp. [Cor], Oscillatoriaceae C > E: *Padina australis*[Dic]	
D vs E	No difference	No difference	No difference
A vs B	No difference	A≠B (**p=0.03**; 98% diss.) Only in A: *Padina australis*[Dic] B > A: *Sargassum* sp. [Fuc]	A≠B (**p=0.03**; 100% diss.) Only in A: *Padina australis*[Dic]
A vs C	No difference	No difference	No difference
A vs D	No difference	No difference	No difference
A vs E	A≠E (**p=0.03**; 71% diss) A > E: Dictyotales E > A: Bryopsidales	A≠E (**p=0.03**; 77% diss.) E > A: *Halimeda opuntia*[Bry] A > E: *Padina australis*[Dic]	No difference
B vs C	No difference	No difference	No difference
B vs D	No difference	B≠D (**p=0.03**; 100% diss.) only in D: *Lyngbya* sp. [Osc], *Padina australis*[Dic], *Halodule pinifolia* [Ali]	No difference
B vs E	No difference	B≠E (**p=0.04**; 100% diss.) Only in E *Halimeda opuntia*[Bry], *Halimeda discoidea*[Bry], *Padina australis*[Dic]	B≠E (**p=0.03**; 100% diss.) Only in E *Halimeda discoidea*[Bry], *Padina australis*[Dic]
C vs D	No difference	No difference	No difference
C vs E	C≠E (**p=0.03**; 80% diss.) only at E: Bryopsidales C > E: Dictyotales	No difference	No difference
D vs E	D≠E (p = **0.03**; 87% diss.) only at D: Oscillatoriales E > D: Bryopsidales(E)	D≠E (**p=0.02**; 90% diss.) only in E: *Halimeda opuntia*[Bry] only in D: *Lyngbya* sp.[Osc], *Halodule pinifolia* [Ai] E > D: *Padina australis*[Dic]	No difference
In 10m:	no differences (all p > 0.13)	no differences (all p > 0.13)	no differences (all p > 0.13)

and in June at sites E and I.

TSS were generally higher across sites in May with an average of 1.8 ± 0.5 mg L^{-1} compared to in June at 0.8 ± 0.3 mg L^{-1} whereas they peaked in surface waters of site E with 1.5 ± 0.1 mg L^{-1} (Fig. 4, Appendix Table 4). Interestingly, highest Chl *a* concentrations were also found at site E in June, peaking in surface waters with 3.31 μg L^{-1}, reflecting a high photosynthetic and thus phytoplankton activity at this site. These values correspond to the lower water transparency at this site (Fig. 3).

3.1.3. Sediment nutrient characteristics

Significant differences were found in the chemical composition of the sediment among sites (Fig. 5, Appendix Table 5).

The offshore site D, in particular, was characterized by low C_{org} and N levels, which were significantly higher at site A and also peaked at site E. In contrast, total C was lowest at site A, followed by site E, with significant differences to site B. The isotope ratios showed highest average values of $\delta^{15}N$ of about 5.8 at site A, which also shows the lowest $\delta^{13}C$ values of about −18.9. *Vice versa* the outer site D showed the lowest $\delta^{15}N$ values of about 4.4 and the highest $\delta^{13}C$ values of about 17.6 (Appendix Fig. 1). Also the visual characterization of sediment composition showed differences between sites (Appendix Table 1). Grain sizes were overall finest in site D, followed by site II, in contrast to the rather coarse sediments of sites E, C and B. All sites showed considerable amounts of carbonate grains from fragmented coral skeletons, but also (parts of) gastropod and bivalve shells, crustaceans, sea urchin spines and photosymbiotic large benthic foraminifera were omnipresent. Depth-related trends were also apparent in most sites, excluding site D. Sediment grain sizes seemed to increase with and higher amounts of sponge spicules along with lower amounts of large benthic foraminifera with increasing depth. However, since these observations are solely based on visual inspections of bulk sediments, they were subjective and should be scientifically tested in future studies.

3.2. Macrophytic diversity, species distribution, and abundance

During the study a total of 87 macrophyte species were encountered in the subtidal (>1 m water depth) within the Nha Trang Bay (Table 1), including 19 species of Chlorophyta (2 orders: Bryopsidales, Cladophorales), 22 species of Ochrophyta (3 orders: Dictyotales, Ectocarpales, Fucales), 41 species of Rhodophyta (11 orders: Bonnemaisoniales, Ceramiales, Corallinales, Gelidiales, Gigartinales, Gracilariales, Halymeniales, Nemaliales, Nemastomatales, Peyssonneliales, Rhodymeniales) and 2 species of Tracheophyta (1 order: Alismatales). In addition, 2 species of bloom forming filamentous cyanobacteria (1 order: Oscillatoriales) were collected and included in the investigations.

The highest species number was observed at site E (54 spp.), followed by sites A (40 spp.), B (34 spp.) and D (32 spp.), and the less diverse site C (29 spp.). Comparing the composition of the different species, clear differences were visible between sites D and E and the sites A, B and C, which showed about 60% similarity, visualized in the NMDS in Fig. 6A.

Considering the occurrence of different species, only 6 species were highly abundant and frequently found at every survey site (Table 1, frequency), including the one Chlorophyta *Halimeda discoidea*, the two Rhodophyta *Amphiroa fragilissima* and *Tricleocarpa cylindrical*, and the three Ochrophyta *Padina australis*, *Sargassum mcclurei* and *Turbinaria ornata*. The majority (59%) showed a patchy distribution, whereas 32 species can be considered as rare, as they were only encountered at one survey site during sampling activities. Furthermore, five additional species found at sites I (*Dichotomaria marginata, Claudea batanensis, Halimeda macroloba*) and II (*Chondria armata, Rhipidosiphon javanensis*) were not sampled at any other site during the present study.

During the quantitative survey in June 2019, a total of 54 species, belonging to 18 macrophyte orders (3 Chlorophyta, 3 Ochrophyta, 10 Rhodophyta, 1 Cyanobacteria and 1 Tracheophyta) were collected (Table 1). Species richness was generally higher in 3 m across all sites (Fig. 6B, Appendix Table 6) particularly in Site A and E, with a species richness of 10.3 ± 3.2 and 10.5 ± 1.3, respectively. This was also due to the appearance of the Chlorophyta *Caulerpa chemnitza, Bornetella nitida* and the Rhodophyta *Gracilaria arcuata, Liagora* sp., *Asteromenia anastomosans* and an unidentified cyanobacteria mat (Oscillatoriaceae), which was solely sampled and identified at site E during the survey.

Padina australis (Fig. 1D) was the only taxon from the six most frequently found (see above) in survey quadrats at all sites, peaking in abundance at site A with 78 ± 70 g dry weight m^{-2} at 6 m water depth

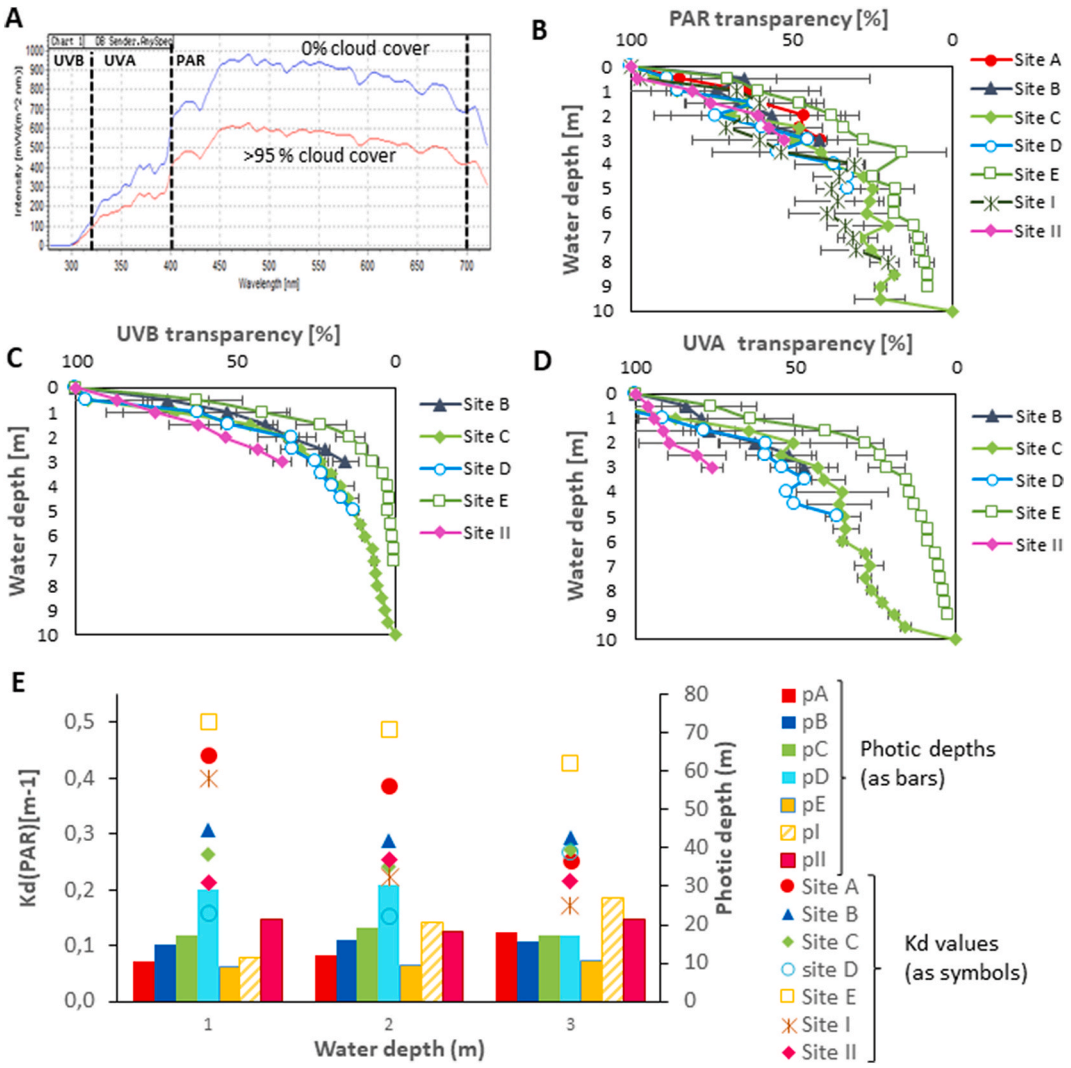

Fig. 3. Natural light regime A) Cloud affected differences in light regime measured with Ramses at surface level under clear sky (0% cloud cover) and >95% cloud cover on June 12 at noon at site B; Underwater light regime calculated as %-surface radiation over depth gradient at different sites in June 2019: B) PAR (400–700 nm measured with LICOR; C) UV-B (280–320 nm) and D) UV-A (320–400 nm), both measured with Ramses; E) Kd and euphotic depths calculated over the first 3 m depth gradient at different sites.

Table 3
Comparison of biomass vs. photo quadrat cover data. 1-way PERMANOVA and subsequent pairwise and SIMPER analyses showing differences in taxa composition and species richness in macroalgal communities grown at 3 m at different sites. Data based on Bray-Curtis similarities of relative percentage abundance data, calculated from biomass and cover data, root-transformed prior to analyses. All taxa contributing 60% of observed dissimilarity are listed, giving the site with highest abundance in brackets. Significant results are indicated in bold.

		Biomass			Cover		
Source	df	Pseudo-F	p	Pairwise	Pseudo-F	p	Pairwise
Taxa composition							
Site	4	3.0466	**0.001**	A≠B (54% Diss.): 22% HAL (B), 18% TUB (A), 15% AMP (A), 13% SAG (A) A≠C (76% Diss):17% PAD (C), 17% TUB (A*), 11% AMP (A), 10% SAG (A), 9% HAL (A) B≠C (71% Diss.): 26% HAL (B), 20% PAD (C); 12% SAG (B), 10% *Dictyosphaeria* (C)	7.399	**0.001**	A≠B (56% Diss.): 22% TUB (A), 21% HAL (B), 15% SAG (A), 12% AMP (A) A≠C (77% Diss):26% PAD (C), 15% SAG (A),15% TUB (A) B≠C (88% Diss.): 35% PAD (C), 30% HAL (B)
Res	9						
Species richness (S)							
Site	4	1.8	0.263	n.s.	9.163	**0.005**	A > all other
Res	9						

(Fig. 6C).

Overall macroalgal composition differed strongly between sites (Table 2, Fig. 6D). Strongest differences within and between sites were observed in the shallow subtidal at 3 m water depth, whereas variability and differences in community composition vanished with increasing depth. Most sites differed from each other at 3 m depth.

The highest macrophyte standing stock was observed in the shallow waters at sites A and B and was mainly composed by members of the

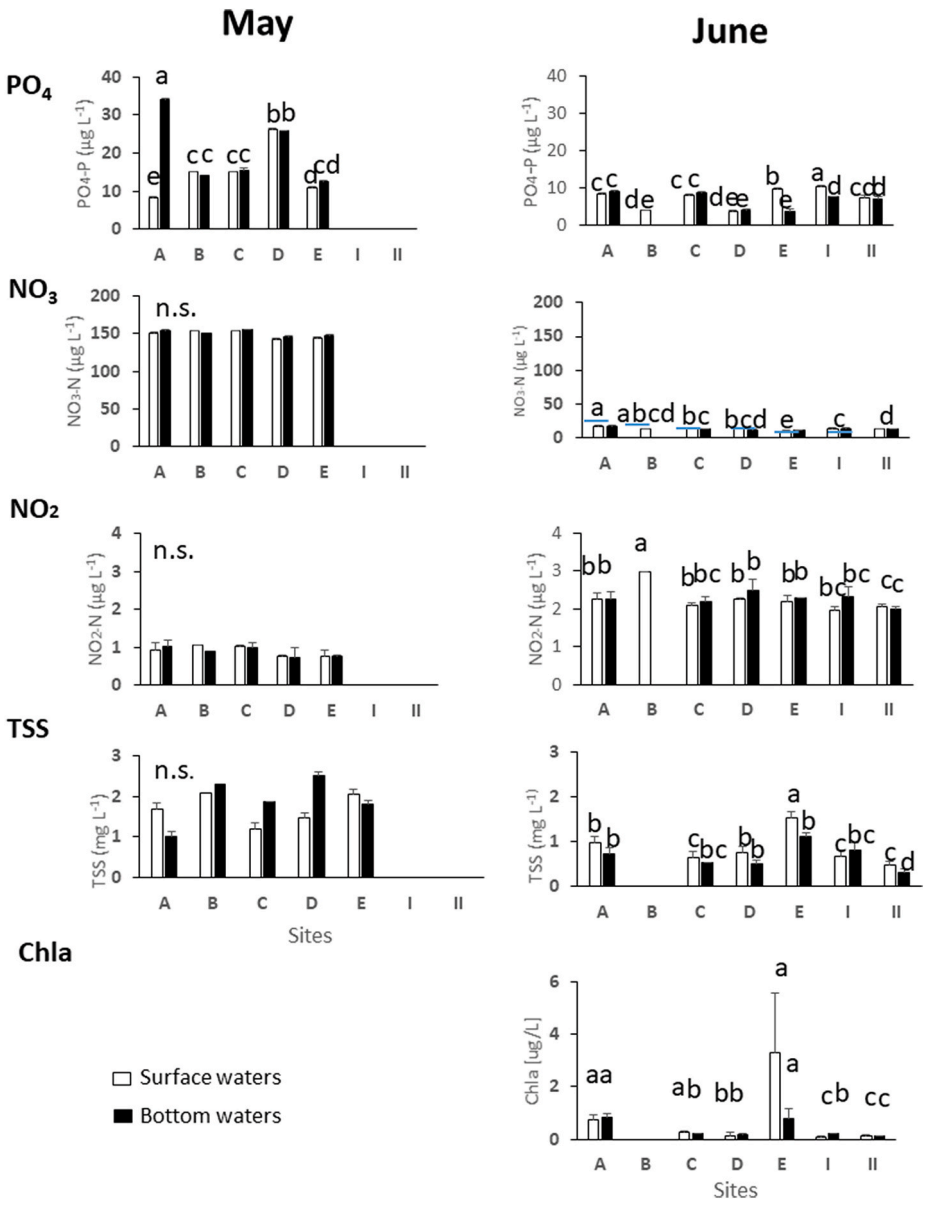

Fig. 4. Water chemistry. Measurements of surface (white bars) and bottom (black bars) water at the different sampling sites (A-E, I-II) in May and June 2019 for water column nutrient concentrations total suspended matter (TSM), and Chlorophyll *a* (Chla; only in June). Letters indicate differences between the different treatments based on PERMANOVA subsequent pairwise comparisons, generated from Euclidean distances with Monte Carlo corrections.

brown algal order Fucales (e.g. *Sargassum* spp., *Turbinaria* spp.) (Table 2). A narrow but biomass-rich *Sargassum* band was also observed at site B between 3 and 5 m water depth (photo shown in Fig. 1 C). Differences between site A and site B were mainly due to higher abundances of *Turbinaria ornata, Amphiroa* spp. and *Padina australis* at site A and a higher amount of *Halimeda discoidea* at site B (Table 2).

Compared to site B, site E also showed high abundances of the Bryopsidales, mainly composed by *Halimeda opuntia*. In addition site E showed a generally low amount of Ochrophyta, but a higher number in Rhodophyta, such as *Chondrophycus parvipapillatus*, which was only found at this site (Tables 1 and 2, Fig. 6D). Compared to the other sites, site C had a significantly low diversity ($S = 4.3 \pm 1$) at 3 m (Fig. 6B) and was characterized by *Padina australis* dominating the macrophytic community in the shallow waters. Next to their significant difference in standing stock (Fig. 6D) the pristine site D strongly differed (90% dissimilarity) from site A, mainly to its low amount of Corallinales (*Amphiroa* spp.) which were lacking in the quantitative survey (Table 2). Also site D was mainly composed by Bryopsidales and Fucales, but differed in species composition from site B, as *Halimeda velasquezii* and *Sargassum* sp. were mainly found at site B and *Halimeda* spp. and *Sargassum polycystum* at site D. Furthermore, the occurrence of a cyanobacteria *Lyngbya* sp. bloom, covering wide parts of the shallows subtidal at site D caused significant differences in the composition between site D and site B, as well as site D and site E at 6 m water depths (Table 2).

Significant differences between water depths were repeatedly caused by the algal orders Bryopsidales (*Halimeda* spp.), Corallinales (*Amphiroa* spp.), and Nemaliales (*Galaxaura* spp.), which showed a clear depth related decrease (Table 1, Table 2). Fucales (*Sargassum* spp., *Turbinaria ornata*) were present at 3 m at every site but did not show a clear depth decrease, whereas Dictyotales (*Padina australis*) showed higher abundances in 6 m water depth at site A. Overall observed differences between depth and sites were prominent not only on species but also on algal order level, whereas hardly any difference was found in the frequent taxa (Table 1).

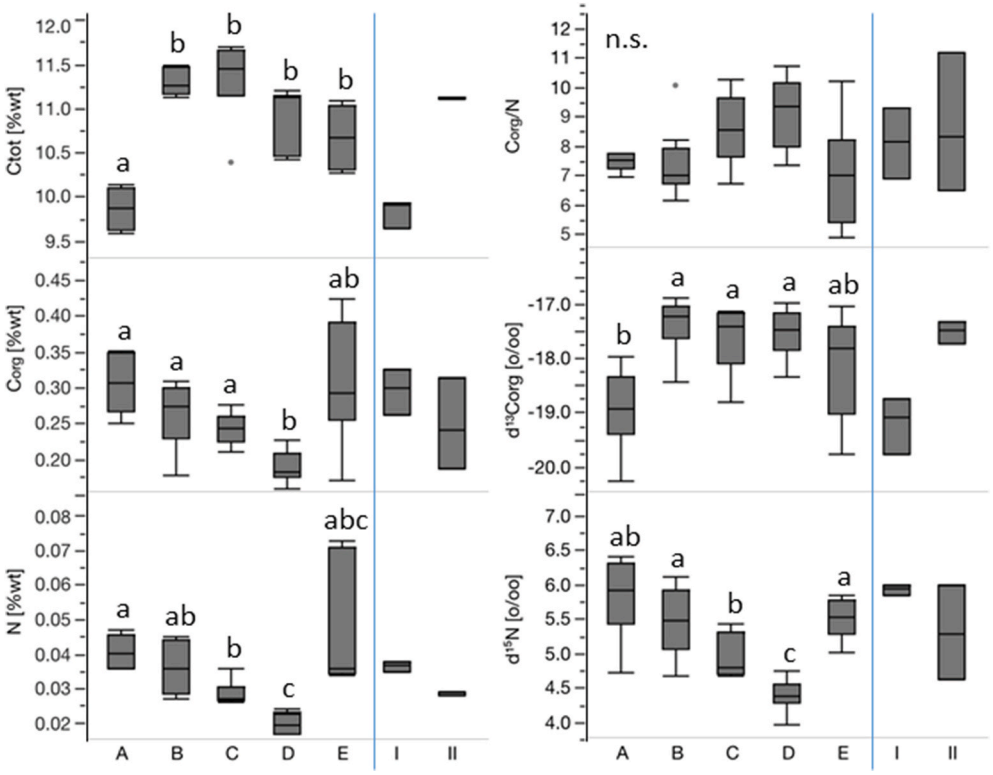

Fig. 5. Sediment chemistry. Box-plot showing mean sediment total C and N and organic C (C_{tot}, C_{org}, N, C_{org}/N) and isotopic carbon and nitrogen composition sampled in across sites (A-E, I, II) in June 2019. Data showing outcome of samples taken from 3, 6 and 10 m (n = 1) at each site. Small letters indicate significant differences calculated with PERMANOVA based on Euclidean distances. Sites I and II were excluded from statistical analyses as only samples from one depth each were available (8 and 10 m, respectively).

3.2.1. Method comparison for quantifying relative abundance using biomass vs. photo-quadrat sampling methods

Through our analysis we showed that the non-destructive photo quadrat method was generally equivalent to the more quantitative, but destructive biomass sampling method to identify presence and abundance of taxa, with a few exceptions (Fig. 7, Table 3).

A total of 15 macroalgal taxa were classified for this analysis, including 1 Chlorophyta: *Halimeda*, 7 Ochrophyta: *Chnoospora* (CHN), *Dictyota* (DIC), *Lobophora* (LOB), *Padina* (PAD), *Sargassum* (SAG), *Turbinaria* (TUB), 6 Rhodophyta: *Amphiroa* (AMP), *Asparagopsis* (ASP), *Galaxaura* (GAL), *Gracilaria/Hydropuntia* (GRA), *Jania* (JAN), *Laurencia* (LAU), *Hypnea* (HYP), *Tricleocarpa* (TRI). In addition, 3 functional taxa groups were included: a) Algal turf (TURF), b) Coral (COR) and c) Invertebrates (INV) and 3 different substrates were discriminated: i) Coral rubble (CR), ii) Rock (R) and iii) Sand (S). *LAU* and *HYP* were hard to distinguish on pictures. Rare species (present in <2 of the 14 quadrats) were underestimated (*JAN, TRI*) or not captured by analyses (*ASP, CHN, GAL, GRA*) on pictures. For the more abundant taxa (present in >2 of the 14 quadrats) the upright growing thalli of *SAG, TUB, PAD, HAL, AMP* were mainly captured, whereas more crustose growing taxa like *DIC* or *LOB* were often overseen and thus underestimated.

Nevertheless, the main differences in 3 m taxa composition were similarly captured in biomass and cover data indicating the same significant site differences (Fig. 7A and B, Table 3). The causative taxa in both analyses (causing 60% of observed differences) also remained the same, with exception of the occurrence of *Dictyosphaeria* in the biomass samples of site C (Replicate 4), which was not recorded in the photographs but significantly contributed to the dissimilarity between the sites B and C in the biomass data. Comparing the outcome of the two methodologies the highest discrepancies were observed in the analyses of the pristine site D, visualized in the NMDS (Fig. 7C). This is mainly due to the fine sediment composition at this site (Appendix Table 1), which became easily dispersed and affected the quality of the underwater photography.

Species richness (S) strongly differed between the two analyses, due to lower species numbers in cover data, resulting in different statistical conclusions (Fig. 7D, Table 3). The pronounced differences in S at site E can be explained by an observed higher number of cryptic and patchy growing taxa (up to 6 species difference at site E). In addition, the dimensionality of substrate also seemed to play a crucial role, as different taxa that only appear in the biomass samples grew closely attached on coral rubble and stones or were partly overlaid with sediment and thus were not visible in photographs.

3.3. Potential abiotic drivers shaping environments and macrophytic composition

Comparing the different sites at 3 m water depths, ten abiotic factors were highly correlated (r > 0.75) with the PCO axes, explaining 39.2% and 23.9% of total variation among sites (Fig. 8A and B).

There were clear differences due to the elevated pH (Appendix Table 2) and sediment nutrient load (C_{org}, N, Fig. 5) at site A and E, as well as in the bottom waters of site A (NO_3–N June, PO_4–P June/PO_4–P May) (Fig. 4). The high planktonic activity (Turb, TSS, Chl *a*) at site E and the high transparency (%UVB, %UVA) at site C and D are distinctly indicated in the plot (Fig. 8A and B). Additionally, the estuarine driven salinity gradient (Fig. 2C) clearly separated the different sites.

Considering the potential effect of environmental parameters on the macrophytic composition, a total of eight abiotic factors (water temperature, salinity, pH, Chl *a*, HDO, NO_2–N in May, PO_4–P and NO_3–N in June) were highly correlated (r > 0.75) with the PCO axes, explaining 29.1% and 20.7% of total variation between the different species compositions among sites (Fig. 8C and D). Interestingly, despite playing a minor role in shaping the different site related environments, temperature (Fig. 2B) seemed to play a major role for the macrophytic taxa, as it was the only factor visible in both data sets (Fig. 8C and D). Elevated water temperatures (≥31.5 °C) correlated clearly with site D and E at 3 m depth, where macrophytic composition did not differ (Table 2). In addition the estuarine impact seemed to play a crucial role, as seen by a high correlation with salinity (Fig. 2C). This was also correlated with the

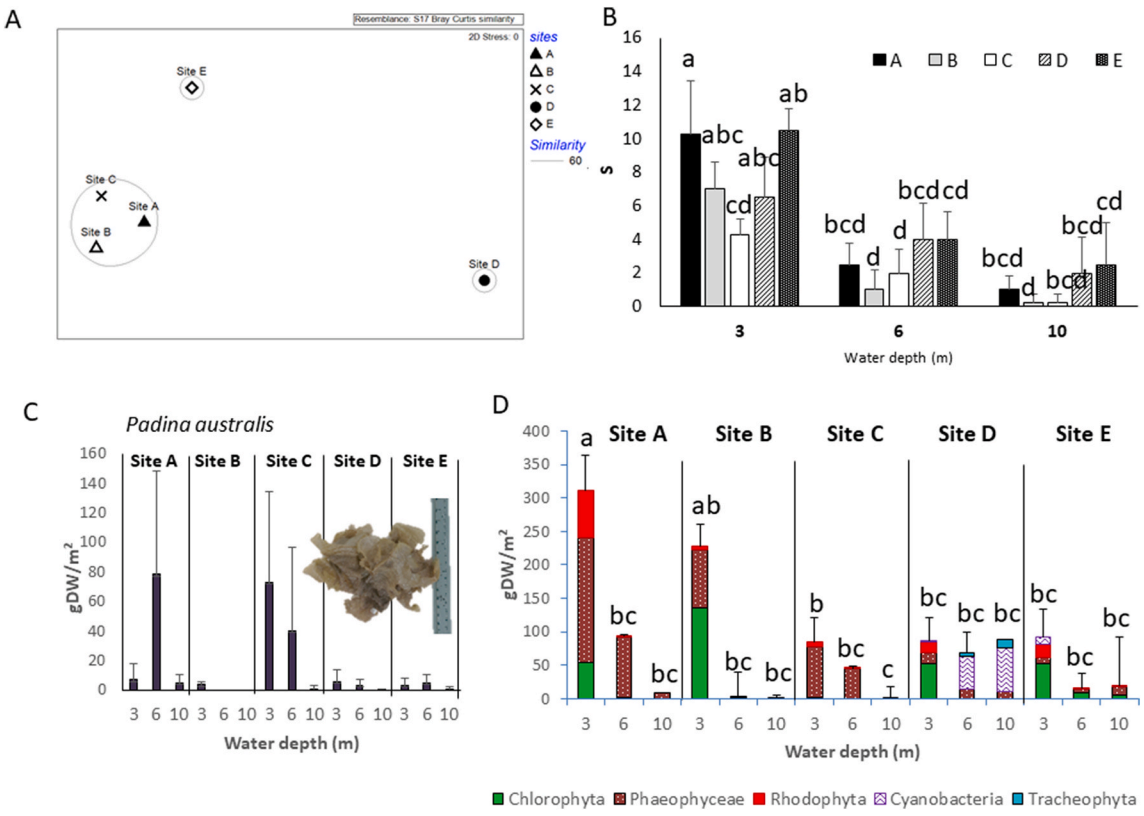

Fig. 6. Macrophyte composition and diversity. A) Non-metric multidimensional scaling plot (NMDS) showing similarities in macrophyte species composition between different sampling sites (A–E) based on overall species presence during qualitative survey. Data based on Bray Curtis distances calculated from log-transformed biomass and non-transformed species presence data. Results of cluster analyses are given showing results for 60% similarity (straight line); B) Species richness (S) during quantitative survey at the different sampling sites. Data showing differences in water depths (3, 6 and 10 m) at the different sites (A–E). Significant differences identified in subsequent PERMANOVA pairwise comparisons are indicated with small letters. Standard deviation is provided; C) Average biomass (based on dry weight) of the frequently found Ochrophyta *Padina australis* and D) of different macrophyte groups calculated from dried material collected in 0.25 m^2 quadrats (n = 4).

offshore sites C and D; whereas higher nutrient loads (PO_4–P June, NO_2–N May, NO_3–N June), Chl *a*, pH, and HDO (Fig. 4, Appendix Table 2) were more strongly correlated with the macrophytic community at site A (Fig. 8C).

4. Discussion

The present study investigated seasonal macrophyte diversity and abundances in Nha Trang Bay, Viet Nam by combining a qualitative and quantitative macroalgal survey approach with correlation of taxa distributions to environmental and water quality parameters.

4.1. Observed macrophyte diversity and patchiness

From the observed 86 species, only six species were repeatedly found at all sites and only one, *Padina australis*, was quantifiable at all sites, and by far the most abundant macrophyte in the upper subtidal zone in our study. This observed remarkable patchiness in macrophyte distribution supports the reported high diversity (Titlyanov et al., 2015b) and underlines the potential importance of the highly abundant brown algae. With a worldwide distribution in tropical to warm temperate seas the genus *Padina* represents one of the abundant key taxa in tropical regions (Silberfeld et al., 2013). From 53 confirmed species (Guiry and Guiry, 2021) only 6 species are previously reported for Viet Nam, namely *P. antillarum, P. australis, P. boryana, P. minor, P. gymnospora* and *P. tetrastromatica* (Nguyen, 2015; Titlyanov et al., 2015b), whereas in the present study we only observed 3 species (*P. australis, P. minor, Padina* sp.). These discrepancies may be due to the morphological species similarity which requires further molecular approaches to better distinguish them apart (Silberfeld et al., 2013; Ni-Ni-Win et al., 2021). Next to its apparently important ecological role the abundant alga, *P. australis,* is frequently used in SE Asia to prepare gelatin-like sweetmeat and salad (Pereira, 2016), provides a source of immune-stimulating fucoidan (Yuguchi et al., 2016) and is reported to show a variety of promising anti-oxidant and anti-bacterial properties (Hongayo et al., 2012; Latifah et al., 2019; Yu et al., 2019). Furthermore, the associated microbiome of *Padina* might provide a source of interesting secondary compounds. This has recently been shown in Vietnamese waters, for which anti-cancer acting Ophiobolin derivates were extracted from the Ascomycete *Aspergillus flocculosus*, which epiphytized an unknown *Padina* species collected at 10 m water depth (Choi et al., 2019). In this context, the highly abundant *Padina australis* provides an interesting and still understudied natural resource which potentially will be harvested along the Vietnamese and neighboring coasts in the future.

In contrast to *P. australis*, most of the other 85 encountered macrophytic species were characterized by strong patchiness, leading to strong differences in taxa composition between the sites. The observed variations in biomass and changes in taxa composition raise the question of the responsible environmental factors apparently shaping this complex algal mosaic.

Comparing the ratios of the species encountered in this study to the reported 327 macrophyte species encountered in past surveys from 2002 to 2010 from intertidal to 5 m water depth (Titlyanov et al., 2015a), we found a relatively higher number of Ochrophyta (27% instead of 16%) in the present sampling, while relative numbers of Rhodophyta (50% instead of 54%) and Chlorophyta (23% instead of 30%) were much

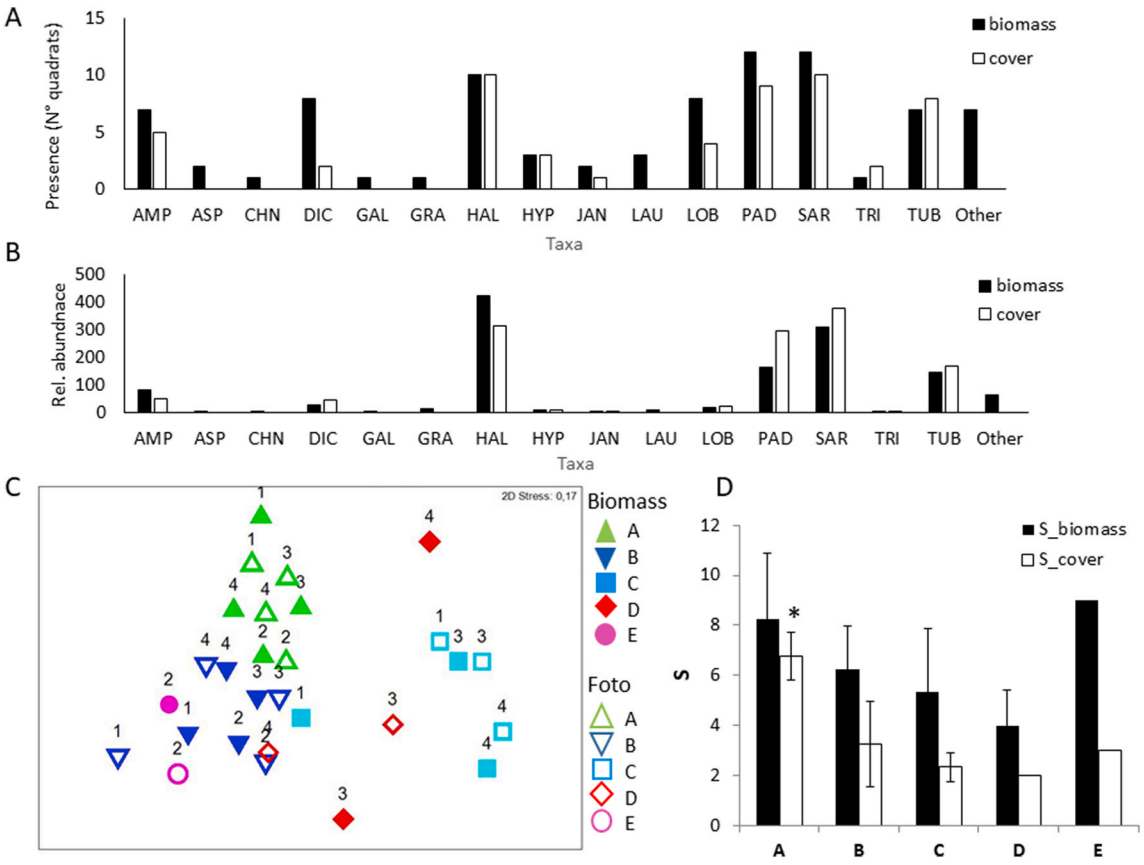

Fig. 7. Comparison of two methods of macroalgal relative abundance quantification based on biomass measurements in dry weight m^{-2} (black bars, filled symbols) and relative %-cover (white bars, empty symbols) based on photograph analyses. Macroalgae were grouped into most abundant taxa while Cryptic taxa were compiled in a single taxon (other). A) Record of the presence of different taxa within all analyzed quadrats for each method, B) Relative total abundance of different taxa, calculated by summing up relative abundance data, calculated as percentage contribution of individual taxa to each analyzed community, C) NMDS visualizes differences in taxa composition between the different 3 m sites (A–E), based on calculations from biomass (filled symbols) and photo (empty symbols) data. Numbers indicate replicate numbers. Data based on relative %-abundances calculated from biomass and cover; D) species richness calculated for different sites using the two methods. Asterisk indicate significant higher value within cover data set.

lower.

These discrepancies can be partly related to the sampling approach, as the present survey did not include the shallower intertidal sites, which are known to favor the development of a rich Chlorophyta (e.g. Ulvales, Cladophorales) algal community (Titlyanov et al., 2015a). Furthermore, monsoon driven seasonal differences in abundance and presence of different algal taxa is a common observed phenomena (Mayakun and Prathep, 2005; Rani et al., 2015; Titlyanov et al., 2019). Thus Rhodophyta like *Phycocalidia vietnamensis* and *Grateloupia* spp are known to bloom at the end of the monsoon season, eventually profiting from elevated nutrient supply by riverine input, and are collected in the short time from January to February (Tsutsui et al., 2005).

Besides nutrients, light plays a crucial role in supporting algal biomass growth. Measured Kd (PAR) values $< 0.5\ m^{-1}$ reflect the outcome of a study of Lund-Hansen et al. (2010), who measured Kd along the Nha Phu estuary, situated in the North of our study area, where in dry seasons especially the impact of the northward flowing outlet of the Cai river contributed to a high organic matter content and higher Kds were measured in wet monsoon conditions. Notably, the calculated and measured PAR values indicated a euphotic depth below 10 m for all sites. As there were generally no depth related differences in nutrient concentrations, the decline in macroalgal biomass below this depth may be due to light limitation. Other factors not measured, but potentially influencing macroalgal distribution and abundance with depth could be differences in hydrodynamics or substrate type (Fricke et al., 2011; Peteiro and Freire, 2011).

The Nha Trang Bay provides complex hydro- and morphodynamics driven by a diurnal tidal regime, seasonal storm and monsoon activities (Nguyen and Tran-Thanh, 2014). Monthly dynamics in nutrient data were visible in the present dataset, representing potential impacts due to seasonal monsoon or upwelling activities. In fact upwelling dynamics can be found year-round in the area of Nha Trang (Hein, 2008), peaking in intensity with velocities about 10^{-1}-10^{-2} cm s^{-1} from June to August (Bui, 2004).

4.2. *Environmental characteristics of the different sites and their macrophyte community*

Overall, the estuarine impact was clearly reflected in the measured environmental differences between the sites. Next to the pronounced differences in surface salinities, especially sediment data, which archive environmental signatures integrated over longer time scales, indicate differences in nutrient supply.

4.2.1. *Sites A, B and I - estuarine impacted sites with high Fucales standing stocks*

The measured low salinity and elevated pH and Chl *a* values in surface waters were possibly related to monsoon activities, as 0.4 mm rainfall was registered for the day and strong (5 m s^{-1}) SSE winds reinforced the high tidal flow (Nguyen and Tran-Thanh, 2014), pushing estuarine waters in the direction to site A and elevating phytoplankton activity. Observed strong differences between the outer site D and close

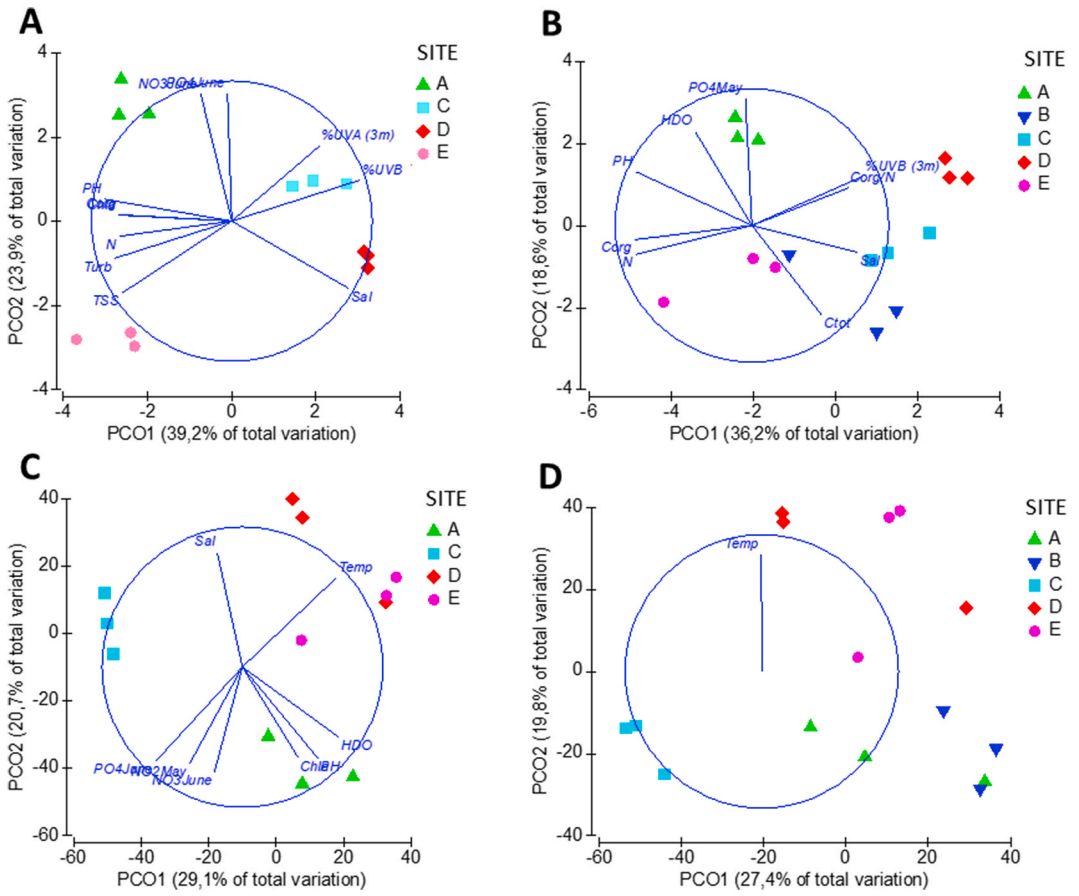

Fig. 8. Principal coordinates (PCO) analyses showing differences between the different survey sites (A–E) in A-B) environmental data and C-D) taxa composition encountered at 3 m water depth. Data based on normalized environmental and log-transformed biomass abundance data, respectively. Due to lacking biochemical data at site B, plots A and C) showing reduced site comparison (excluding site B) considering all available environmental data, including: water temperature, pH, salinity, HDO (mg/l), %UVB, %UVA and %PAR all measured or calculated for 3 m; nutrient concentrations for PO_4–P, NO_3–N and at NO_2–N, as well as TSS and Chl *a*, measured in bottom waters in May and June, respectively; and sediment data. Plots B) and D) present a reduced environmental data set (excluding nutrients and Chl *a* data) comparing all sites. Pearson correlation vectors, representing environmental data, are superimposed as supplementary variables ($r > 0.75$). The length and direction of the vectors represent the strength and direction of the relationship.

to estuary site A, as indicated by elevated C_{org} and N contents, and depleted $\delta^{13}C$ ratios, reflected a stronger terrestrial influence at site A. This has been confirmed by other studies in Vietnamese estuaries (Tue et al. 2011, 2012, 2012; Ellengaard et al., 2014). In contrast to these studies which show $\delta^{13}C$ values below −25‰ indicative of high inputs of compounds from mangrove ecosystems, however, the ratios between −20 and −18‰ detected in site A are still within the range of marine phytoplankton dominated systems (Tue et al., 2011; Rumolo et al., 2011; Ellegaard et al., 2014), suggesting that most of the elevated load of organic matter was produced *in situ* and likely related to the former usage of this location as a lobster farm. This site is also characterized by elevated $\delta^{15}N$ ratios around 6‰, which correlates with increased nitrogen concentrations and may be suggestive of wastewater input (Cole Ekberg et al., 2004). However, despite the stable isotope values indicating enhanced anthropogenic impacts at site A, the detected values are still within a range typical for organic matter of marine origin in sediments, as summarized in Rumolo et al. (2011). Due to the high similarity in sediment parameters, very similar conditions of elevated anthropogenic eutrophication and land-based impacts can be expected at site I, and are likely supporting the rich seasonal macroalgal blooms this underwater plateau, referred to as Bai Can Lon ("Great Bank"), is known for. In contrast to site A, site B seems to be more marine influenced but still receives elevated higher nutrient input possibly due to the close by coastal activities, as reflected in the sediment data with higher total carbon and $\delta^{13}C$ ratios.

Overall site A and B showed a diverse and biomass rich macrophyte community dominated by members of the brown algal Fucales (*Sargassum* spp., *Turbinaria ornata*), the green algal Bryopsidales (*Halimeda* spp.) and the red algal Corallinales (*Amphiroa* spp.) in the shallow waters and high numbers of the brown algal Dictyotales *Padina australis* in the deeper (≥6 m) waters. At the deeper site I dense stands of *Stypopodium zonale* were observed which were also collected at site A.

With about 36 species and variations reported, *Sargassum* provides a highly diverse taxon in the Nha Trang Bay (Titlyanov et al., 2015b). The estuarine driven higher nutrient load seems to be responsible for the development of high diverse brown algal standing stocks at site A, B and I. Strong dependence of *Sargassum* beds on seasonal nutrient supply were also shown in other studies (Hoang et al., 2016). In Nha Trang, *Sargassum* beds showed highest biomass from July to August at Bai Can Lon (site I). Therefore, the annually harvesting season for *Sargassum* at Bai Can Lon is from May to October as reported by Nguyen (1997). Due to rising harvest activities and additional anthropogenic perturbations (e.g. increasing coastal constructions) the *Sargassum* beds in the Nha Trang Bay strongly decreased over the past decades (Nguyen and Nguyen, 2011) and hardly any *Sargassum* stock were observed, when scouting at site I. Next to different *Sargassum* species, *Turbinaria ornata* also showed interesting high anti-oxidative properties (Kelman et al., 2012). *Stypopodium zonale* has proven to provide interesting bioactive properties, e. g. for treating protozoan caused skin infections (Leishmaniasis) (Soares et al., 2016). Overall, the growing interest in Fucoidan

related products (Bui et al., 2007; Thanh et al., 2012) might intensify the anthropogenic pressure on these and other so far abundant Ochrophyta in the future.

4.2.2. Site E – estuarine site with adjacent lobster farms and high macrophyte diversity

Situated close to the outlet of the Cua Be estuary, in close proximity to floating lobster farms, site E was characterized by lower surface salinities, high particulate load and an elevated phytoplankton activity in surface waters. The sediment at site E was also characterized by high $\delta^{15}N$ values, N and C_{org} concentrations, but interestingly, $\delta^{3}C$ ratios were not significantly depleted. This may be due to great variations between depth at this site, with considerably higher $\delta^{13}C$ (and $\delta^{15}N$) ratios in 3 and 6 compared to 10 m depth, while C_{org} and N concentrations clearly peaked in 6 m depth. The high variability in sediment parameters indicates a mixed marine terrestrial influence as observed in other estuaries close by (Ellegaard et al., 2014; Tue et al., 2011), which can be explained by the close proximity to the floating lobster farms, causing high nutrient availability in the upper water column. This enhances phytoplankton production and, hence, increases turbidity and organic matter production at this site. This is likely to reduce light penetration into greater depths, which apparently affects the local benthic community. Actually, studies from different sites, including the Nha Trang Bay, reported a strong impact of marine cage cultures on nutrient levels and turbidity (Du, 2015; Huang et al., 2011). This corresponds to the significantly higher TSS and Chl *a* levels in surface waters measured in our survey which, in combination with $\delta^{13}C$, indicate high marine phytoplankton productivity.

Consequently, compared to the outer site D, the Kd was nearly twice as high and the underwater light level more reduced, with less than 18% UVB, 32% UVA and 17% PAR at site E. Interestingly, despite the observed high turbidity and reduced light, site E showed high species richness comparable to site A, but was composed of a completely different algal community dominated by *Halimeda opuntia* and a variety of other Chlorophyta (e.g. *Caulerpa* spp., *Bornetella nitidia*) and Rhodophyta (*Acanthophora spicifera, Leveillea jungermannioides, Gelidiella acerosa, Gracilaria arcuata, Asteromenia anastomosans*) with taxa only encountered in the quadrats of this site. This formed a diverse but low biomass stock overall. Interestingly some of these species, like *Acanthophora spicifera*, *Gelidiella acerosa, Gracilaria arcuata or Caulerpa racemosa*, belong to commercialized taxa, commonly harvested for food and other purposes in the area (Titlyanov et al., 2012). This raises the question how far the lobster raising (or culturing) activities, next to their input of fertilizing nutrients, might affect the composition of the adjacent benthic habitat.

4.2.3. Site D - sheltered pristine site with seagrass beds and Lyngbya blooms

In contrast to the three nearshore sites, sediment parameters of sites C, D and II indicate less terrestrial and anthropogenic impacts, and characterize them as more marine influenced.

Site D represents the most pristine site in sediment and water parameters, reaching maximum salinity and showing generally low nutrient (besides a PO_4–P peak observed in May), TSS and Chl *a* concentrations, minimum sedimentary organic matter contents and stable isotope signatures, indicating marine influenced conditions, which remained quite stable across depths. The observed mixed seagrass beds composed of *Halodule pinifolia* and *H. major* indicated a more undisturbed character of this site. Sensitive to environmental changes, many of these fragile meadows disappeared from Vietnamese waters over the past decades (Luong et al., 2012; Vo et al., 2020). Nevertheless, the very shallow and enclosed morphology of the bay might restrict water exchange and could thereby cause stressful conditions during summer months for the shallow-dwelling benthic community. In fact, the transparent waters showed the highest temperatures peaking with >31.5 °C in the upper 3 m, which potentially triggered the formation of an observed dense benthic *Lyngbya* bloom, covering various substrates in the shallow depths. These are known to produce a variety of bioactive compounds including some high effective phycotoxins that cause skin irritations and inflammations (e.g. swimmers itch), and can even be hepatoxic or neurotoxic, especially when ingested (e.g. by consuming of infested seaweed) or inhaled (e.g. as aerosols) (Chlipala et al., 2010; Osborne et al., 2001). Consequently, these seasonal blooms could provide potential serious harm for the coastal ecosystem, but might also offer an interesting source for further bioactive substances.

4.2.4. Sites C and II - remote sites with low macrophyte diversity

Site C, close to the small island Hòn Môt, situated in a more remote location, with transparent waters, a steep rocky shore and a sandy gently dropping bottom. The macrophyte community was less diverse as at the other site, similar in species presence to site A and B and surprisingly did not differ in the quantitative survey from site C. *Padina australis* clearly dominated the macrophytic communities, reaching standing stocks comparable to site A. Sediment provided a heterogeneous composition, composed of different sized foraminifera intermixed with coarse carbonate fragments from different organisms and some siliciclastic grains. Notably, 10 m samples also showed a very thin layer of fine greyish-green material.

The remote site II, situated on the slope of the far out Hon Dung Island, also showed a heterogeneous sediment composition and low macrophyte abundances. Interestingly, scouting along the slope, some additional species were encountered, e.g. in addition to the delicate green fan-shaped *Rhipidosiphon javensis* also the red *Chondria armata* occurred, which is known as source of a variety of bioactive compounds, like domoic acid-related alkaloids and triterpene polyethers (Jiang et al., 2014). Domoic acid, which was first extracted and named after the Japanese name for *C. armata* "doumoi" (Takemoto and Daigo, 1958) is produced by some Rhodophyta (*Alsidium*, *Amansia*, *Chondria*, *Digenea*, *Vidalia*) and diatom genera (*Pseudo-nitzschia*, *Amphora*, *Nitzschia*) and is known as a causative agent of Amnesic shellfish poisoning (ASP) caused by consumption of contaminated shellfish (Hambright et al., 2014). In fact *Chondria armata* has been employed for more than 1000 years in Japan to eliminate intestinal worms. Next to the potent anthelminthic and anti-insect properties, potential anti-cancer applications are also currently under development (Gerwick, 2017; Hamada et al., 2020). Given the high bioactivity of the well-studied *C. armata* and the recorded presence of additional five species in the Nha Trang Bay (*C. baileyana, C. dangeardii, C. repens, C. simpliciuscula, C. ryukyuensis*) (Titlyanov et al., 2015a), the potential in this rather cryptic growing group is high. Nevertheless, despite the observed patchiness in our study, care has to be taken as members of this genus, like *C. tumulosa* were recently reported to start overgrowing Hawaiian coral reefs (Sherwood et al., 2020).

4.3. Conclusions

Given the observed prominent differences in macroalgal standing stock and diversity within the shallower waters of the Nha Trang Bay, and the observed depth related decrease in diversity and biomass, we recommend to continue seasonal monitoring in 3 m water depths to cover a full year cycle. The applied combination of quantification (via photo-quadrats) and scouting (via random species picking) helped to increase the recorded macrophyte species number at surveyed sites by about 33%, whereas the use of underwater photographs should be restricted to clear waters where they reliably captured comparative information on main community differences. In this way they can provide a valuable tool to non-destructively extend cost effective underwater macrophytic community surveys.

Based on the findings of the present study a macroalgal-based survey within the Nha Trang Bay should consider seasonality, and therefore should be conducted at the beginning and at the end of the dry season. In addition, future surveys a) can be concentrated on the shallower 3 m water depth, b) should also include contrasting sites and c) need to be

accompanied by different environmental measurements, including physicochemical properties of the water column, nutrient concentrations, light intensity and potentially light spectra to better understand how changing environmental conditions in the region may impact future standing stock of macroalgae, biodiversity and distribution. Furthermore, considering the observable decrease of the economically harvested natural *Sargassum* stocks in the Nha Trang bay, it is also important to continue further research into macroalgal harvest rates to determine the potential impact on this natural resource and implement sustainable resource use practices.

CRediT authorship contribution statement

A. Fricke: Conceptualization, Methodology, Investigation, Formal analysis, Project administration, Writing – original draft. **X.V. Nguyen:** Methodology, Investigation, Formal analysis, Project administration, Writing – review & editing. **M. Stuhr:** Methodology, Investigation, Formal analysis, Software, Writing – review & editing. **T.D. Hoang:** Methodology, Investigation, Formal analysis. **V.H. Dao:** Resources, Supervision. **M.D. Tran:** Methodology, Investigation. **T.S. Pham:** Resources, Supervision. **H.C. Le:** Investigation, Project administration, (permits). **M.H. Le:** Supervision, Project administration, (permits). **Q.L. Pham:** Resources, Supervision. **M. Schmid:** Methodology, Investigation, Writing – review & editing. **A. Kunzmann:** Methodology, Investigation, Writing – review & editing. **A. Gärdes:** Funding acquisition, Writing – review & editing. **J. von Hagen:** Resources, Supervision. **M. Teichberg:** Supervision, Funding acquisition, Project administration, Methodology, Investigation, Writing – review & editing.

Declaration of competing interest

The authors declare that they have no known competing financial interests or personal relationships that could have appeared to influence the work reported in this paper.

Acknowledgements

This research was under the frame of the project TroMaCos (Tropical Macroalgae for the use of Natural Cosmetics) financed by Merck KGaA. MS was supported through a Minerva Post-doc Fellowship. We thank student assistants from IO and NITRA, as well as Ulrich Pint from the ZMT scientific dive team for helping with algal and environmental sample collections and analysis. We thank Jessica Schiebe for her patience and support in analyzing the underwater photos.

Appendix A. Supplementary data

Supplementary data to this article can be found online at https://doi.org/10.1016/j.ecss.2021.107460.

References

Abbott, I.A., Fisher, J., McDermid, K.J., 2002. Newly reported and revised marine algae from the vicinity of Nha Trang, Vietnam. Taxonomy of economic seaweeds with reference to some pacific species. Vol. VIII. I. A. M. Abbott, K.J. Oceanographic institute, Nha Trang, Vietnam. Vietnam: California Sea Grant College 8, 291–321.

Bui, H.L., 2004. Some typical hydrodynamic characteristics of the sea of Vietnam and adjacent Waters. In: Williams, K.C. (Ed.), In Spiny Lobster Ecology and Exploitation in the South China Sea Region Institute of Oceanography. Nha Trang, Vietnam, pp. 44–48.

Bui, L., Ngo, B., Nhut, N., Pham, T., Tran, V., 2007. Studies on Fucoidan and its production from Vietnamese brown seaweeds. Asean Journal on Science and Technology for Development 22, 371–380.

Chlipala, G.E., Pham, H.T., Nguyen, V.H., Krunic, A., Shim, S.H., Soejarto, D.D., Orjala, J., 2010. Nhatrangins A and B, aplysiatoxin-related metabolites from the marine cyanobacterium *Lyngbya majuscula* from Vietnam. J. Nat. Prod. 73, 784–787.

Choi, B.-K., Trinh, P.T.H., Lee, H.-S., Choi, B.-W., Kang, J.S., Ngoc, N.T.D., Van, T.T.T., Shin, H.J., 2019. New Ophiobolin derivatives from the marine fungus *Aspergillus flocculosus* and their cytotoxicities against cancer cells. Mar. Drugs 17, 346.

Cole Ekberg, M., Valiela, I., Kroeger, K., Tomasky, G., Cebrian, J., Wigand, C., McKinney, R., Grady, S., Silva, M., 2004. Assessment of a d 15 N Isotopic method to indicate anthropogenic eutrophication in aquatic ecosystems. J. Environ. Qual. 33, 124–132.

Diaz-Pulido, G., McCook, L.J., 2004. Effects of live coral, epilithic algal communities and substrate type on algal recruitment. Coral Reefs 23, 225–233.

Doan Dung, L., 2007. The Marine Protected Area of Nha Trang Bay, Vietnam. Initial Trends in Resource Status and Utilization (2002-2005). Department of Aquatic Bioscience University of Tromsø, Tromsø.

Du, H., 2015. The assessment of eutrophication in coastal waters under the influences of sea-cage farm activities for the degradation of surrounding coral reef ecosystem in Nha Trang Bay. In: Vietnam. Conference: APN International Conference on: "Developing Life-Supporting Marine Ecosystems along the Asia-Pacific Coasts - a Synthesis of Physical and Biological Data for the Science-Based Management and Socio-Ecological Policy Making".

Du, H.T., Kunzmann, A., 2015. The sediment load and deposition by river discharge and their relation to organochlorine pesticides pollutants in the sediment bottom of Nha Trang Bay, Vietnam. Ocean Sci. J. 50 (2), 455–466.

Ellegaard, M., Nguyen, N.T.G., Andersen, T.J., Michelsen, A., Nguyen, N.L., Doan, N.H., Kristensen, E., Weckström, K., Son, T.P.H., Lund-Hansen, L.C., 2014. Temporal changes in physical, chemical and biological sediment parameters in a tropical estuary after mangrove deforestation. Estuar. Coast Shelf Sci. 142, 32–40.

FAO, 2018. The Global Status of Seaweed Production, Trade and Utilization. Globefish Research Programme, Rome, p. 120.

Fricke, A., Titlyanova, T.V., Nugues, M.M., Bischof, K., 2011. Depth-related variation in epiphytic communities growing on the brown alga *Lobophora variegata* in a Caribbean coral reef. Coral Reefs 30, 967–973.

Fricke, A., Teichberg, M., Nugues, M.M., Beilfuss, S., Bischof, K., 2014. Effects of depth and ultraviolet radiation on coral reef turf algae. J. Exp. Mar. Biol. Ecol. 461, 73–84.

Fricke, A., Kihara, T.C., Hoppenrath, M., 2017. Studying mesoalgal structures: a non-destructive approach based on confocal laser scanning microscopy. Bot. Mar. 60, 181–195.

Gerwick, W.H., 2017. Plant Sources of Drugs and Chemicals, Reference Module in Life Sciences. Elsevier.

Gnanavel, V., Roopan, S.M., Rajeshkumar, S., 2019. Aquaculture: an overview of chemical ecology of seaweeds (food species) in natural products. Aquaculture 507, 1–6.

Guiry, M.D., Guiry, G.M., 2021. AlgaeBase. World-wide electronic publication, National University of Ireland, Galway. https://www.algaebase.org. searched on [June 25 2020].

Ha, T., Huong, L., Cuong, L., Tuan, N., Chi, H., Hang, T., Nghi, D., Ly, D., Imbs, A., Long, P., 2019. Evaluation of biological activities of some seaweed and seagrass species in the coastal area of Vietnam. J. Mar. Sci. Technol. 19, 405–414.

Hamada, T., Kobayashi, K., Arima, N., Tani, F., Vairappan, C.S., Onitsuka, S., Okamura, H., 2020. Two cytotoxic squalene-derived polyethers from the Japanese red alga *Chondria armata*. Nat. Prod. Res. 1–6.

Hambright, K.D., Zamor, R.M., Easton, J.D., Allison, B., 2014. Algae. In: Wexler, P. (Ed.), Encyclopedia of Toxicology, third ed. Academic Press, Oxford, pp. 130–141.

Hanelt, D., Tüg, H., Bischof, K., Groß, C., Lippert, H., Sawall, T., Wiencke, C., 2001. Light regime in an Arctic fjord: a study related to stratospheric ozone depletion as a basis for determination of UV effects on algal growth. Mar. Biol. 138, 649–658.

Hein, H., 2008. Vietnam Upwelling - Analysis of the Upwelling and Related Processes in the Coastal Area off South Vietnam.

Hoang, T.C., Cole, A.J., Fotedar, R.K., O'Leary, M.J., Lomas, M.W., Roy, S., 2016. Seasonal changes in water quality and *Sargassum* biomass in southwest Australia. Mar. Ecol. Prog. Ser. 551, 63–79.

Hongayo, M., Larino, R., Malingin, D., 2012. Antibacterial and antioxidant effects of brown alga *Padina australis* Hauck crude extract. IAMURE International Journal of Science and Clinical Laboratory 2.

Huang, Y.-C., Hsieh, H., Huang, S.C., Meng, P.-J., Chen, Y.-S., Keshavmurthy, S., Nozawa, Y., Chen, C.A., 2011. Nutrient enrichment caused by marine cage culture and its influence on subtropical coral communities in turbid waters. Mar. Ecol. Prog. Ser. 423, 83–93.

Jiang, S., Kuwano, K., Ishikawa, N., Yano, M., Takatani, T., Arakawa, O., 2014. Production of domoic acid by laboratory culture of the red alga *Chondria armata*. Toxicon 92, 1–5.

Kelman, D., Posner, E.K., McDermid, K.J., Tabandera, N.K., Wright, P.R., Wright, A.D., 2012. Antioxidant activity of Hawaiian marine algae. Mar. Drugs 403–416.

Kirk, J.T.O., 1994. Light and Photosynthesis in Aquatic Ecosystems, 2 ed. Cambridge University Press, Cambridge, pp. 252–270.

Kohler, K., Gill, S., 2006. Coral Point Count with Excel extensions (CPCe): a Visual Basic program for the determination of coral and substrate coverage using random point count methodology. Comput. Geosci. 32, 1259–1269.

Kunzmann, A., et al., 2012. River Reef Impact Studies I (RRIS I): Reef Responses to Changing Water Temperatures.

Latifah, L., Soekamto, N., Tahir, A., 2019. Preliminary study: *Padina australis* Hauck's antibacterial activity and phytochemical test against pathogenic shrimp bacteria. J. Phys. Conf. 1341, 022005.

Le, N., Nguyen, H., 2010. Rong Câu Việt Nam, Nguồn Lợi Và Sử Dụng. Hanoi,i. Natural Science and Technology Publishing HouseHanoi, p. 242.

Littler, M.M., Littler, D.S., 1999. Epithallus sloughing: a self-cleaning mechanism for coralline algae. Coral Reefs 18, 204-204.

Lund-Hansen, L.C., Hai, D.N., Lam, N.N., Nielsen, M.H., 2010. Optical properties of a tropical estuary during wet and dry conditions in the Nha Phu estuary, Khánh Hòa Province, south-east Vietnam. Hydrobiologia 644, 207–216.

Luong, C., Thao, N., Komatsu, T., Dac Ve, N., Tien, D., 2012. Status and threats on seagrass beds using GIS in Vietnam. Proceedings of SPIE - The International Society for Optical Engineering 8525, 12.
Mayakun, J., Prathep, A., 2005. Seasonal variations in diversity and abundance of macroalgae at samui island, surat thani province, Thailand. Songklanakarin J. Sci. Technol. 27.
Nguyen, H.D., 1997. Sargassaceae in Vietnam, Resource and Utility. Agriculture Publishing House, p. 190.
Nguyen, H.D., 2007. Fucales, Flora of Vietnam. Science and Technological Publish House, Hanoi, pp. 1–117.
Nguyen, V.T., 2015. Seaweed Diversity in Vietnam, with an Emphasis on the Brown Algal Genus *Sargassum*. Department of Biology. Ghent University, Ghent, p. 191.
Nguyen, X.-V., Nguyen, H.D., 2011. Re-assessment of *Sargassum* Beds at Hon Chong Area, vol. 41. Publications of the Seto Marine Biological Laboratory, Nha Trang Bay, Vietnam, pp. 63–69.
Nguyen, L., Tran-Thanh, T., 2014. A Study on Hydrodynamics and Morphodynamics of the Nha Trang Bay, Khan Hoa Province A.Conference. IAHR-APD, Hanoi.
Nguyen, T., Le, N.H., Lin, S.-M., Steen, F., De Clerck, O., 2013. Checklist of the Marine Macroalgae of Vietnam. Botanica Marina, 56.
Nguyen, X.V., Lau, V.K., Nguyen-Nhat, N.T., Nguyen, T.H., Phan, K.H., Dao, V.H., Ho-Dinh, D., Hayashizaki, K., Fortes, M.D., Papenbrock, J., 2021. Update of seagrass cover and species diversity in Southern Viet Nam using remote sensing data and molecular analyses. Regional Studies in Marine Science, 101803.
Ni-Ni-Win, T., Hanyuda, A., Kato, H., Shimabukuro, M., Uchimura, H., Kawai Tokeshi, M., 2021. Global diversity and geographic distributions of *Padina* species (Dictyotales, Phaeophyceae): new insights based on molecular and morphological analyses. J. Phycol. 57 (2), 454–472.
Osborne, N., Webb, P., Shaw, G., 2001. The toxins of *Lyngbya majuscula* and their human and ecological health effects. Environ. Int. 27, 381–392.
Parsons, T.R., Maita, Y., Lalli, C.M., 1984. Manual of Chemical and Biological Methods for Seawater Analysis. Pergamon Press, p. 173.
Pereira, L., 2016. Edible Seaweeds of the World. CRC Press, Coimbra, Portugal.
Pereira, R.C., da Gama, B.A.P., 2008. Macroalgal chemical defenses and their roles in structuring tropical marine communities. In: Amsler, C.D. (Ed.), Algal Chemical Ecology. Springer Berlin Heidelberg, Berlin, Heidelberg, pp. 25–55.
Peteiro, C., Freire, O., 2011. Effect of water motion on the cultivation of the commercial seaweed *Undaria pinnatifida* in a coastal bay of Galicia, Northwest Spain. Aquaculture 314, 269–276.
Pham-Hoang, H., 1969. Marine Algae of South Vietnam. Trung tâm học liệu, Saigon, p. 511.
Puk, L., Cernohorsky, N., Marshell, A., Dwyer, J., Wolfe, K., Mumby, P., 2020. Species-level effects of herbivorous fishes on the establishment of the macroalga *Lobophora* on coral reefs. Mar. Ecol. Prog. Ser. 637.
Rani, V., Jawahar, P., shakila, R., 2015. Seasonal variation in biomass and distribution of brown seaweeds (phaeophyceae) in gulf of mannar, tamilnadu, India. Bioscan 10, 1123–1129.
Rumolo, P., Barra, M., Gherardi, S., Marsella, E., Sprovieri, M., 2011. Stable isotopes and C/N ratios in marine sediments as a tool for discriminating anthropogenic impact. J. Environ. Monit. : JEM 13, 3399–3408.
Sherwood, A.R., Huisman, J.M., Paiano, M.O., Williams, T.M., Kosaki, R.K., Smith, C.M., Giuseffi, L., Spalding, H.L., 2020. Taxonomic determination of the cryptogenic red alga, *Chondria tumulosa* sp. nov., (Rhodomelaceae, Rhodophyta) from Papahānaumokuākea Marine National Monument, Hawai'i, USA: a new species displaying invasive characteristics. PloS One 15 e0234358.
Silberfeld, T., Bittner, L., Fernández-García, C., Cruaud, C., Rousseau, F., de Reviers, B., Leliaert, F., Payri, C.E., De Clerck, O., 2013. Species diversity, phylogeny and large scale biogeographic patterns of the genus *Padina* (Phaeophyceae, Dictyotales). Phycology 49, 130–142.
Soares, D.C., Szlachta, M.M., Teixeira, V.L., Soares, A.R., Saraiva, E.M., 2016. The brown alga *Stypopodium zonale* (Dictyotaceae): a potential source of anti-*Leishmania* drugs. Mar. Drugs 14 (9), 163.
Takemoto, T., Daigo, K., 1958. Constituents of *Chondria armata*. Chem. Pharmaceut. Bull. 6, 578b–580.
Tanna, B., Mishra, A., 2018. Metabolites unravel nutraceutical potential of edible seaweeds: an emerging source of functional food. Compr. Rev. Food Sci. Food Saf. 17, 1613–1624.
Teichberg, M., Fricke, A., Bischof, K., 2013. Increased physiological performance of the calcifying green macroalga *Halimeda opuntia* in response to experimental nutrient enrichment on a Caribbean coral reef. Aquat. Bot. 104, 25–33.
Thanh, T., Van, T.T.T., Hidekazu, Y., Hiroshi, U., 2012. Fucoidan from Vietnam *Sargassum swartzii*: isolation, characterization and complexation with bovine serum Albumin. Asian J. Chem. 24, 3367–3370.
Titlyanov, E.A., Titlyanova, T.V., Pham, V.H., 2012. Stocks and the use of economic marine macrophytes of Vietnam. Russ. J. Mar. Biol. 38, 285–298.
Titlyanov, E., Titlyanova, T., Belous, O., 2015. Checklist of the marine flora of Nha Trang Bay (Vietnam, South China Sea) and decadal changes in the species diversity composition between 1953 and 2010. Bot. Mar. 58, 367–377.
Titlyanov, E., Titlyanova, T., Huang, H., Skriptsova, A., Xu, H., Li, X.-B., 2019. Seasonal changes in the intertidal and subtidal algal communities of extremely and moderately polluted coastal regions of Sanya Bay (Hainan Island, China). J. Mar. Sci. Eng. 7, 93.
Tkachenko, K., 2015. Ecological status of coral communities in the island area of the Nha Trang Bay (Vietnam). Russ. J. Ecol. 46, 456–462.
Tsutsui, I., Huynh, Q.N., Nguyên, H.D., Arai, S., Yoshida, T., 2005. The Common Marine Plants of Southern Vietnam. Japan Seaweed Association, p. 250.
Tue, N.T., Hamaoka, H., Sogabe, A., Quy, T.D., Nhuan, M.T., Omori, K., 2011. The application of δ13C and C/N ratios as indicators of organic carbon sources and paleoenvironmental change of the mangrove ecosystem from Ba Lat Estuary, Red River, Vietnam. Environmental Earth Sciences 64, 1475–1486.
Tue, N.T., Ngoc, N.T., Quy, T.D., Hamaoka, H., Nhuan, M.T., Omori, K., 2012. A cross-system analysis of sedimentary organic carbon in the mangrove ecosystems of Xuan Thuy National Park, Vietnam. J. Sea Res. 67, 69–76.
Vo, T.-T., Lau, K., Liao, L., Nguyen, X.-V., 2020. Satellite image analysis reveals changes in seagrass beds at Van Phong Bay, Vietnam during the last 30 years. Aquat. Living Resour. 33, 4.
Yu, K.-X., Sn, N., Ng, C.H., 2019. Antimibrobial potential of *Padina australis* and *Sargassum polycystum* against respiratory infections causing Bacteria. International Journal of Medical Toxicology & Legal Medicine 22, 138–141.
Yuguchi, Y., Tran, V.T.T., Bui, L.M., Takebe, S., Suzuki, S., Nakajima, N., Kitamura, S., Thanh, T.T.T., 2016. Primary structure, conformation in aqueous solution, and intestinal immunomodulating activity of fucoidan from two brown seaweed species *Sargassum crassifolium* and *Padina australis*. Carbohydr. Polym. 147, 69–78.